Construction and Building Materials 342 (2022) 127975

Contents lists available at ScienceDirect

Construction and Building Materials

journal homepage: www.elsevier.com/locate/conbuildmat

Review

Application and modelling of Shape-Memory Alloys for structural vibration control: State-of-the-art review

Alireza Tabrizikahou [a,*], Mieczysław Kuczma [a], Magdalena Łasecka-Plura [b], Ehsan Noroozinejad Farsangi [c], Mohamamd Noori [d], Paolo Gardoni [e,1], Shaofan Li [f]

[a] Institute of Building Engineering, Poznan University of Technology, Piotrowo 5, 60-965, Poznan, Poland
[b] Institute of Structural Analysis, Poznan University of Technology, Piotrowo 5, 60-965 Poznan, Poland
[c] Faculty of Civil and Surveying Engineering, Graduate University of Advanced Technology, Kerman, Iran
[d] Department of Mechanical Engineering, California Polytechnic State University, CA, United States
[e] Civil and Environmental Engineering Department, University of Illinois at Urbana-Champaign, Urbana, IL 61801, United States
[f] Department of Civil and Environmental Engineering, The University of California, Berkeley, CA, 94720, United States

ARTICLE INFO

Keywords:
Shape Memory Alloy
Structural seismic response
Vibration
Passive control
Active control
Review

ABSTRACT

One of the most essential components of structural design for civil engineers is to build a system that is resistant to environmental conditions such as harsh chemical environments, and catastrophic disasters like earthquakes and hurricanes. Under these circumstances and disturbances, conventional building materials such as steel and concrete may demonstrate inadequate performance in the form of corrosion, deterioration, oxidizing, etc. Shape Memory Alloys (SMAs) are novel metals with distinct features and desirable potential to overcome the inadequacies of existing construction materials and enable the structure to tolerate disturbances more efficiently. Shape Memory Effect (SME) and Pseudoelasticity (PE) have been the most attractive characteristics that scientists have focused on among the various features that SMAs exhibit. The SME enables the material to retain its original shape after severe deformation, whereas the PE behaviour of SMAs provides a wide range of deformation while mitigating a substantial amount of susceptible stresses. These behaviours are the consequence of the phase transformation between austenite and martensite. Many investigations on the modelling and application of SMAs in structural systems to endure applied dynamic loadings in the form of active, passive, and hybrid vibration control systems have been undertaken. The focus of this paper is to present an overview of the SMA-based applications and most frequently employed constitutive modelling, as well as their limits in structural vibration control and seismic isolation devices.

1. Introduction

1.1. Shape memory alloys and structures: a brief review

The purpose of using smart materials for earthquake resistant design is to build a structural system that provides improved mechanical performance while requiring minimal extra mass, energy consumption, or construction expense. In other terms, a smart seismic control system is a technology that reduces or dissipates the destructive effects of earthquake actions on a structure [1]. Smart materials frequently offer innovative features and can be employed to improve mechanical and seismic response performance in structural systems [2].

Shape Memory Alloys (SMAs) are a metallic category of smart materials that may revert to their original undeformed shape after substantial deformations by unloading and/or heating owing to phase transformations between austenite and martensite. Heating (shape memory effect (SME)) or stress reduction (pseudoelasticity (PE)) triggers this reverse phase transformation from martensite to austenite.

Ölander made the first discovery of the SME in 1932, and Vernon coined the term "shape memory" in 1941 [3]. In 1961 Buehler and Wiley [4] observed a series of alloys (Nickel and Titanium) that displayed the shape-memory phenomena while working at the US Naval Ordinance Laboratory in 1961. Because of the combination of various terms, this alloy was called NiTiNOL (Nickel–Titanium and the discovery at Naval Ordinance Lab). These discoveries have sparked a great deal of interest and study into both the properties and the possibly unique applicability in structures.

Due to the numerous advantageous characteristics exhibited by SMAs, such as hysteretic behaviour, excellent re-centring capability, large damping capacity, ability to undergo large deformations, etc, they

* Corresponding author.
E-mail address: alireza.tabrizikahou@doctorate.put.poznan.pl (A. Tabrizikahou).
[1] Director of Mid-America Earthquake Center (MAE).

https://doi.org/10.1016/j.conbuildmat.2022.127975
Received 27 March 2022; Received in revised form 12 May 2022; Accepted 25 May 2022
Available online 8 June 2022

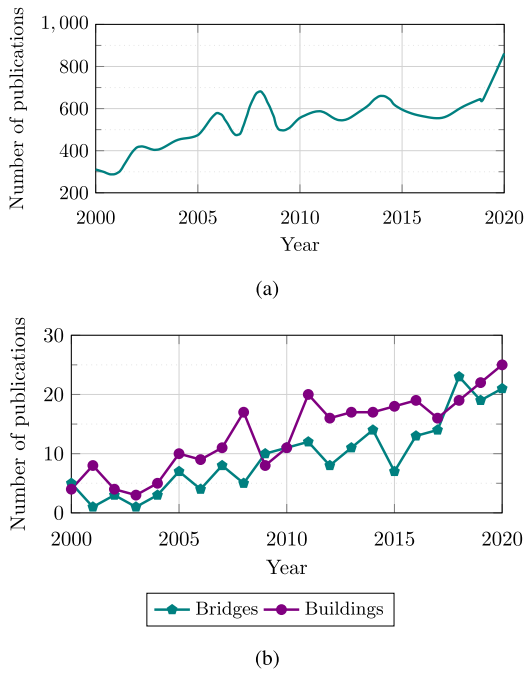

Fig. 1. Number of SMA-related publications between 2000 and 2020; (a) general applications of SMAs; (b) SMA applications in bridge and building engineering.

have been one of the most desirable scientific topics among researchers in recent years for use in civil structures.

SMAs may be utilized in retrofitting and strengthening existing structures, as well as in structural and seismic design [5]. SMAs (particularly Ni–Ti) have been used in the design of civil constructions in structural systems such as beam–column connections, special braces, reinforcing or pre-stressing bar, dissipation dampers, and base isolation systems [6,7].

1.2. Current trends and perspectives

Considerable investigation and development attempts in the field of SMAs have been undertaken in the previous two decades, owing to advancements in materials sciences, laboratory instruments, the use of advanced computational techniques, and a variety of other enhancements. These remarkable developments in research and technology resulted in a better knowledge of phase transformation, simplicity of production and implementation, and the discovery of low-cost alloys with shape-memory behaviour.

The large and escalating number of papers in SMA-related research in recent years attests to this tremendous rise (Fig. 1a). Furthermore, by reviewing these publications on the use of SMAs in buildings and bridge structures, it is clear that there is tremendous progress in these two sectors of study as well (Fig. 1b).

For many years, the comparatively expensive cost of manufacturing and processing SMAs in buildings was one of the material's limits (particularly for Ni–Ti SMA). However, the recent development of low-cost SMAs made mostly of iron (Fe-based SMAs) and copper (Cu-based SMAs) allows SMAs to be used in a greater range of large-scale constructions [8,9]. As a result, the development of low-cost SMAs (based on Fe and Cu) is another important factor in the rising contribution of SMA application in structural engineering [10]. The development of novel materials, in particular, has attracted a lot of attention in recent years due to the growing availability of low-cost equipment, as well as recent advancements in sophisticated manufacturing procedures.

1.3. Critical appraisal of the state-of-the-art and contribution of the present work

Despite the fact that SMAs have been widely implemented in civil engineering structures and that research interest in this area is increasing, there are still a few scientific and practical gaps that must be addressed. Many researchers have attempted to answer these inadequacies, and there have been numerous breakthroughs and innovations in this scientific discipline. As a result, it would be extremely beneficial to compile all of these advancements, as well as the current limitations, into a state-of-the-art review paper to provide a comprehensive overview of this topic to scholars investigating the application and modelling of SMAs in vibration response control of civil engineering structures. Several informative and valuable review articles on the vibration control application and modelling of SMAs have been published during the last two decades. Some of these review studies are briefly presented in this section.

Saadat et al. [11] provided an overview concerning with: (i) Ni–Ti properties (SME, PE and other thermodynamic properties), (ii) modelling (e.g. models by Tanaka [12,13], Niezgódka and Sprekels [14], Müller and Xu [15], Lexcellent and Tobushi [16] and etc.), and (iii) applications for structural vibration control and seismic isolation based on the mechanism used (active, passive and hybrid vibration control).

Desroches and Smith [17] evaluated the different attributes of SMAs (fatigue, strain rate and temperature effect) and their application for seismic design and retrofitting of structures (e.g. wired-based devices, seismic rehabilitation of buildings, and bridge structures).

Wilson and Wesolowsky [18] addressed materials science characteristics, numerical modelling, and thermomechanical behaviour of SMAs pertinent to earthquake design, as well as an examination of the existing development of SMA-based vibration control devices and their application in buildings and bridges. We consider that this study covered a wide variety of topics, with an emphasis on both practical implementation and numerical modelling.

Qian et al. [19] carried out a review on SMA-based structural vibration control in civil engineering. They provided fundamental details concerning the thermodynamic behaviour of SMAs, as well as constitutive models developed by Graesser and Cozzarelli [20,21], and Wilde, Gardoni and Fujino [22]. The researchers next examined the existing seismic applications of SMAs for buildings, taking into account passive, active, and hybrid vibration control mechanisms.

Ozbulut et al. [23] presented an extensive review of seismic applications of SMAs in different types of structures. They reviewed the fundamental features of SMAs, constitutive models, and their use in the seismic design of civil engineering structures. This study, we consider, is one of the most useful review articles on the seismic response control of civil engineering structures using SMAs.

Zareie et al. [24] presented an extensive analysis of current breakthroughs in SMA implementations in civil infrastructures. They proceeded by providing a short overview of the SME and PE characteristics of SMAs, as well as recent developments in building and bridge structures. The significance of this review article may be the classification according to the type of structure (concrete, steel, and timber), as well as the type of system (isolation, bracing, stiffeners and etc.).

Billah et al. [25] evaluated current SMA-based bridge engineering uses, as well as classified the properties of SMAs relevant for the bridge engineering sector, and indicated topics of potential improvement and prospects. The benefit of this work is that it categorizes the application of SMAs in bridge engineering based on the SMA material composition, used properties (SME, PE, energy dissipation and damping) and type of element (bar, wire, tube, etc.). This paper is particularly beneficial for researchers working on the use of SMAs in bridge structures.

We believe that all of the previously stated review articles provide a wide variety of information in this scientific field that will help scholars gain a better understanding of the application of SMAs in civil engineering structures. However, in this paper we attempted to address

the limitations and perspectives of the current state-of-the-art on the topic of vibration control of civil engineering structures using SMA. It was tried to provide a complete review of different aspects of this subject by reviewing the most important properties of SMAs, different types of SMAs and their advantages and shortcomings, categorizing different constitutive models and introducing a few of them comprehensively, and application of SMAs in seismic and vibration control of the different type of civil engineering structures, etc. The following aspects differentiate this research from other review articles:

- evaluating the most current developments, innovations, limits and constraints, and prospects of the use of various types of SMAs in civil engineering constructions (building, bridges, etc.);
- a review of the thermodynamic, physical, SME and PE behaviour, and other properties of several types of SMAs, as well as their effectiveness in vibration control devices in civil engineering structures;
- the important qualities of SMAs for vibration control applications (damping, fatigue, strain rate, and so forth) and how to enhance them (additional alloying component, annealing, etc.);
- categorizing and describing the most often used constitutive models proposed of SMAs for dynamic and seismic design;
- presenting a review of the literature on the use of SMAs in seismic and vibration control systems used in various types of structures (buildings, bridges, etc.) constructed with various materials (concrete, steel and masonry);
- using numerous illustrations of SMA properties, constitutive models, and their application in civil engineering structures to present readers with a clearer vision and comprehension;
- summarizing and assessing the vibration control systems in terms of the SMA deformation mechanisms (SME or PE), cost, constructability, energy dissipation, and effectiveness.

1.4. Article overview

Section 2 explores further the SME and PE behaviour of SMAs in terms of phase transformations and the influence of the thermomechanical stimuli on them. In addition, three types of the most prevalent compositions of Ni–Ti, Cu-based, and Fe-based SMAs are described, and their physical and mechanical characteristics are compared.

When considering dynamic loadings in structural design, several characteristics of the material utilized in the structure are critical. Section 3 presents some of these elements as well as the fundamental features of SMAs that are believed to be critical in the design of seismic response control devices.

Vibration response control systems, in general, adopt passive, active, or semi-active approaches. Section 4 describes the basics of these structural seismic response control systems to assist readers to grasp the information in the following sections.

Many computational methods have been introduced to computationally model the SMA's dynamic behaviour. Section 5 goes through three of the most frequently applied SMA dynamic computational models in a one-dimensional domain.

Many studies have been conducted to determine the advantages and disadvantages of adopting SMA-based vibration control systems in structural components. Section 6 delves deeply into these applications concerning three different approaches of passive, active and semi-active control.

Section 7 highlights the various uses of SMA-based structural control systems, as well as the existing scientific and practical gaps based on the literature, and the prospects of employing SMAs in vibration device systems.

Section 8 briefly concludes the results of the reviewed studies by providing the current scientific and practical gaps and the future possible research areas.

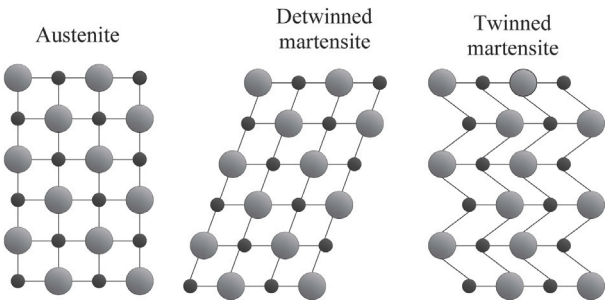

Fig. 2. Crystal orientations in different temperature states of SMAs [26].

2. Fundamental inherent characteristics of shape memory alloys

SMAs, like many other alloys, possess polymorphism, which indicates that they can exist in more than one crystal structure form with the same chemical composition, as illustrated in Fig. 2. The austenite stronger structure (parental phase), is stable at higher temperature and lower stress states. Martensite has a reduced amount of order in its crystal structure, which makes it more stable at lower temperatures and high-stress states.

Fig. 3 depicts the peculiar shape-memory characteristics of SMAs that emerge from reversible martensitic phase transitions. As seen in Fig. 3a, there is some residual strain in the materials after the loading and unloading procedure. When the material is heated above A_s, the twinned martensite begins to transfer to the austenite phase until it reaches A_f, at which point only austenite remains. Afterwards, the austenite is completely converts to twinned martensite by cooling the material from M_s to M_f. These four temperature points are determined by the material composition, manufacturing method, and applied stresses of the SMA. SMAs exposed to temperatures over a specific point of M_d irreversibly distort like any other conventional metal, and stress-induced deformation can occur beyond this point.

The curve in Fig. 3b indicates hysteresis, and the region encompassed by the hysteresis loop corresponds to dissipated energy and therefore to the damping capacity of SMA. According to Duval et al. [27], the residual strain is determined by the temperature at the unloading process. For SMA structural elements both the modelling and the simulation of boundary-value problems are complex and difficult, due to the perceived dissipative character of the deformation process under reversible transformations in the mixture of phases that results in the flag-shaped hysteresis [15,28–31].

SME and PE may be divided into three categories of shape memory characteristics:

- one-way SME that retains a distorted shape after an external force is removed and reverts to its initial state when heated;
- SME with two-way (reversible) memory that remembers its formation at both high and low temperatures. However, it is not widely commercialized due to its poorer recovery compared to the one-way SME for the same material [32] and its proclivity to rapidly degenerating the strain, especially at high temperatures [33];
- pseudoelasticity: With no thermal stimulation, the SMA recovers to its original shape when subjected to mechanical loading at temperatures ranging from A_f to M_d.

Binary (Ni–Ti) and ternary (Ni–Ti–X, where X is an additional alloying agent) nitinol alloys outperformed other SMAs owing to superior characteristics such as shape recovery, pseudoelastic strain, and recovery stress. As a result, it finds usage in a variety of applications, including retrofitting and reinforcing materials, seismic control devices, and self-sensing and -repair elements. However, the substantial manufacture and installation costs of nitinol alloys, as well as their

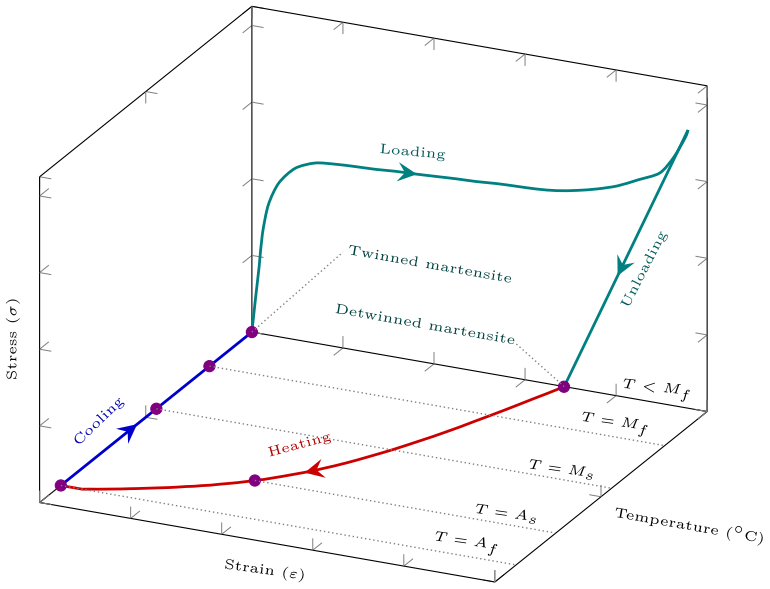

(a)

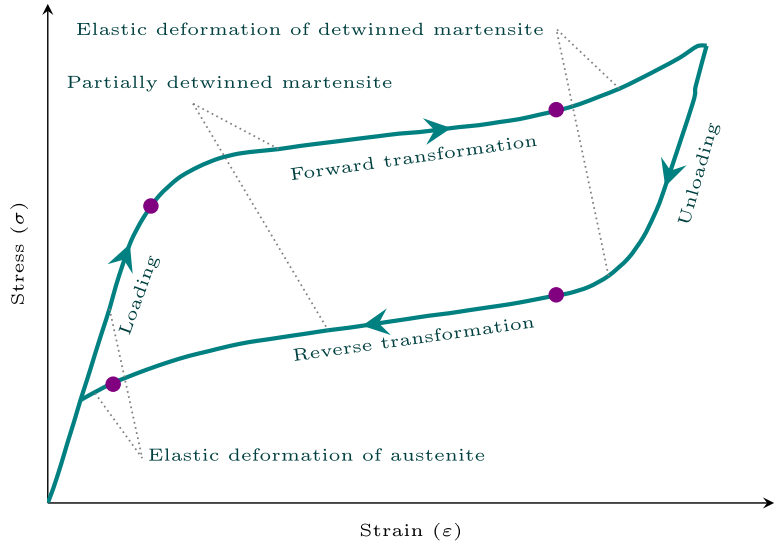

(b)

Fig. 3. Stress–strain–temperature curves for: (a) SME; (b) PE.

extreme temperature sensitivity, have been a detriment to their broader spectrum of use in buildings. Accordingly, there has been a significant effort to develop novel SMAs or modify existing ones to be more cost-effective, such as Cu- and Fe-based SMA.

Sato et al. [8] reported shape memory behaviour in the Fe–30Mn–1Si alloy in 1982. One of the reasons that Fe-based SMAs are intriguing is because the majority share in the composition is iron (Fe, from Latin: Ferrum), which is a cheap and readily available element [10]. Fe-based SMAs can be classified into two categories;

- Fe–Pt, Fe–Pd, and Fe–Ni–Co: with low thermal hysteresis and almost similar martensitic phase transition behaviour to NiTi-NOL, however, Fe–Pt or Fe–Pd alloys are not reported to exhibit pseudoelasticity at room temperature;
- Fe–Ni–C and Fe–Mn–Si: with higher thermal hysteresis, while exhibiting SME.

Among these Fe-based SMAs, Fe–Mn–Si alloys have attracted attention because of their low cost, excellent workability, good weldability, and other remarkable properties.

Binary Cu-based SMAs (from Latin: Cuprum) containing Zn, Al, and Sn, with or without the ternary alloying agent, are desired to owe to their good shape recovery, simplicity of manufacture, and excellent thermal and electrical conductivity. In addition to SME and pseudoelasticity, Cu-based SMAs exhibit Temperature Memory Effect (TME), which is shown after an incomplete reverse martensitic transition [9].

Several engineering properties of Ni–Ti, Fe–Mn–Si and Cu–Al–Ni SMAs are compared to stainless steel in Table 1. The quantities in Table 1 for the specified attributes are based on the findings of several studies in order to present a wide range of information. Furthermore, the range of Ni–Ti quantities provided is governed by the crystal phase (martensite or austenite) and other factors (hardened or fully annealed).

Table 1
Comparison of physical and mechanical characteristics of Ni–Ti, Fe–Mn–Si and Cu–Al–Ni SMAs to stainless steel.

Property	Ni–Ti	Fe–Mn–Si	Cu–Al–Ni	Stainless steel
Density (kg/m^3)	6450–6500 [34]	7200–7500 [35]	7100 [36]	7850 [37]
Poisson's ratio	0.33 [38]	0.359 [39]	0.3 [40]	0.265-0.3 [41,42]
Young's modulus (GPa)	28–83 [43]	160–200 [39]	30-85 [44]	190–120 [37,45]
Specific heat capacity (J/kg °C)	450–620 [46]	540 [47]	500 [48]	420–510 [49]
Thermal conductivity (w/m °C)	8.6–18 [50]	8.4 [47]	30-43 [51]	8.9–16.2 [49]
Ultimate tensile strength (MPa)	895–1900 [52]	680–1200 [53]	1000 [54]	480-1450 [42]
Yield stress (MPa)	70–690 [55,56]	475 [57]	950 [58]	170-850 [59,60]
Yield strain (%)	5–10 [61]	2.5–13 [62]	4-6 [63,64]	0.2-1.6 [65]
Ultimate strain (%)	5–50 [66]	12.4–20 [53]	10-30 [67]	1-40 [65]
Corrosion resistance	Very good [68]	Good [69,70]	Fair [71,72]	Fair [73]
Cost	High [74]	Low [35]	Low [75]	Low
SME	High [76]	Moderate	Low [77,78]	–
Workability	Moderate [79,80]	Low [81]	Good [82]	Good [37]
Fabrication	Low [83]	Good [84]	Moderate [85]	Good [37]
Processing	Demanding [79,86]	Easy [39]	Easy [87]	Easy [37]

Materials used in structural vibration control systems and devices must have specified features and characteristics. These attributes should be consistent with the nature of these systems, which are designed to withstand dynamic and heavy loading conditions. Section 3 thoroughly discusses some of the key aspects and characteristics of SMAs, as well as how they might be enhanced. However, the following observations may be drawn from the data in Table 1:

- since structural elements are frequently susceptible to humidity, severe chemical or environmental conditions, and pollutants, they must be corrosion resistant or insulated. Because Ni–Ti has superior corrosion resistance as compared to other SMAs and stainless steel, it has a wide range of uses in biological and medical applications (however, because nickel is a highly poisonous substance, additional alloying material is being added to the composition to improve corrosion and avoid physiological harm). Other Cu-based and Fe-based SMAs have good corrosion resistance, but many studies are conducted to improve this attribute, such as the impact of alloying components, annealing, employing epoxy, etc.
- another key issue is the mechanical qualities of the materials employed in such structures and systems. In comparison to stainless steel, the reported SMAs exhibit excellent mechanical properties, including high yield and ultimate strain, as well as much greater ultimate tensile strength and yield stress. It allows them to endure extreme-loading situations (they might also dissipate energy and return to their original form with the help of their SME and PE behaviour).
- other essential consideration is the cost and simplicity of manufacture, as well as the material's machinability and processability. Among the SMAs presented, Ni–Ti has comparatively high manufacturing and processing costs with restricted workability (due to its high sensitivity to temperature), but Fe–Mn–Si is an affordable SMA with acceptable workability, making it a more viable SMA for usage in civil engineering constructions.
- in seismic occurrences, the lower weight of the material used reduces the seismic force imposed on the structure. The density of the three proposed SMAs is lower than that of stainless steel, implying that a lower quantity of material may be employed in the structural control system. However, because steel and concrete comprise the majority of the materials used in conventional structures, this factor may not play a significant role in the seismic response control of structures.

3. Basic properties of shape memory alloys

In addition to their shape memory characteristics, SMAs have exceptional material properties that distinguish them from other conventional construction materials. High damping capacity, excellent fatigue resistance, great re-centring ability, etc. are some of the unique characteristics of SMAs that make them viable for the design of structural vibration control systems. Some of these properties are thoroughly discussed in this section.

3.1. Damping

Damping is the process of converting mechanical (kinetic and strain) energies to thermal energy in order to reduce or constrain structural motions or vibrations. This is a measure of a material's efficiency in dispersing a huge quantity of produced external energy through deformations or vibratory response in order to maintain the stability and integrity of a structure [88,89]. Damping is required to lessen the negative impact of ground motions on civil engineering structures, which would otherwise result in the total collapse of such systems [90].

The damping capacity of SMA, which refers to its ability to absorb the vibration energy due to a dynamic response under applied load, determines its potential applications for passive structural control. SMA damping is based on two mechanisms: martensite variations reorientation (SME) and stress-induced martensitic transition of the austenite phase (pseudoelasticity) [91]. Metallic alloys exhibiting the martensitic phase transition have been proven in studies to have a desired damping capacity [92].

Friction is a key mechanism in the damping process, and it can manifest as external friction at the interface of two interacting structural components (at the macro-scale level) or as internal friction within the damping material (at micro-scale level). SMAs have a large damping capacity due to the relatively high internal friction that occurs during the martensitic transition. Lie et al. [93] noted that the martensite damping capability of strained Ni–Ti SMAs varies with annealing temperature and duration. Martensite damping diminishes with a growing number of repetitions under tension–compression cyclical stress, and it continues to equilibrium with more repetition.

Several studies have explored the pre-stressing SMA wires to improve their damping ability. According to several research studies, SMA wires must be pre-tensioned to half of the ultimate strain and cycled about the pre-strained value for producing effective energy dissipation [94–96]. On the other hand, increasing the pre-tensioning may reduce the level of energy dissipation. As a result, in an optimum design, pre-tensioning should be restricted to less than half of the ultimate strain. Dolce and Cardone [97] recommended that the austenite wires should be pre-tensioned to increase energy dissipation. They also examined the damping properties of Ni–Ti bars under torsion in martensite and austenite phases and discovered that the damping capacity of the martensite bar is rather larger than the damping capacity of the austenite bar. It is also worth noting that the mechanical characteristics of a martensite bar are unaffected by loading frequency, but the austenite bar is highly reliant on frequency. This allows both martensite and austenite Ni–Ti bars to perform at a high frequency.

Many variables and conditions influence the material behaviour of SMAs, such as temperature state, loading rate, strain amplitude, number of cycles, and geometry of the shape memory components, making it difficult to derive a general formula for damping capacity values. However, the following formula has been reported in the literature [98] for the Specific Damping Capacity (SDC).

$$\text{SDC}\ (\%) = \Delta w / w \tag{1}$$

where Δw is the dissipated energy and w is the applied energy. For example, the SDC values of Ni–Ti, Cu–Zn–Al and Cu–Al–Ni SMAs are 15%–20%, 30%–85% and 10%–20% respectively [99]. The exact SDC value of these SMAs depends on the frequency and the amplitude.

Equivalent Viscous Damping (EVD) may also be used to assess the energy dissipation performance of specimens in a seismic control mechanism. It is a dimensionless measurement of energy dissipation that is based only on the form of the hysteretic curve, as described below [100]:

$$\text{EVD } (\%) = \frac{W_D}{4\pi W_E} \tag{2}$$

where W_E is the stored energy in a linear system experiencing a comparable maximum displacement and load like those used to calculate W_D, and it correlates with the triangle area of the load–displacement curve of the linear system.

Alaneme et al. [101] investigated the dynamic characteristics, particularly the damping characteristics, of untreated Cu–32Zn–10Sn and Ni-modified Cu–32Zn–10Sn SMAs. The damping capabilities of the 0.4 wt% Ni adjusted CuZnSn alloy for the range of test temperatures were substantially greater than the ranges observed for the untreated and 0.2 wt % Ni adjusted CuZnSn alloys. According to the findings, the optimal compromise of physical and damping characteristics was obtained by micro-alloying CuZnSn alloy with an equivalent of 0.4 wt% Ni.

Ivanić et al. [102] evaluated the influence of various thermal processing mechanisms on the microstructure, damping capabilities, and physical characteristics of CuAlNi SMA. Based on their dynamic-mechanical study, they discovered that specimens following solution annealing and tempering had a better damping capacity.

3.2. Fatigue

Considering that seismic loads have inherent sinusoidal loading nature, the cyclic behaviour and fatigue resistance of SMAs under repeated loading circumstances is essential to whether they are to be employed in seismic applications.

Fatigue is the weakening of the periodic characteristics of SMAs, which is classified into structural and functional fatigue [103,104]. The concentration of microstructural malformations and the development and propagation of fractures until the material splits is referred to as structural fatigue. The progressive deterioration of either SME or damping capability caused by microstructural changes is referred to as functional fatigue. Aside from corrosion, fatigue is another element to consider when aiming for a long life cycle. Temperature, alloy composition, loading type, microstructure, and surface quality are all factors that impact SMA fatigue resistance.

Cyclic loadings cause progressive increases in residual stresses due to microstructural slippage during the stress-induced martensite transition during subsequent cycles. They also cause a decrease in martensite forward stress levels [105,106]. This is followed by a decrease in the stress required to induce reverse transformations, which is less than that required for forwarding phase transformations. As a result, the SMA's hysteresis and energy dissipation are reduced (approximately 40% decrease) [107–111].

DesRoches et al. [112] subjected a Ni–Ti SMA wire and bar (1.8 and 25.4 mm diameter) to cyclical loadings. They both demonstrated outstanding pseudoelastic behaviour (see Fig. 4). However, the SMA wire outperformed the SMA bars in terms of strength and damping. Section size has no effect on re-centring capabilities based on residual stresses. Cyclic strain amplitudes larger than 6% resulted in a loss of damping and re-centring capacity.

Janke et al. [99] outlined several requirements for improving fatigue resistance. First, they found out that the high mechanical strength of austenite and martensite improves the SMAs' fatigue characteristics. Alloys having relatively soft austenite, such as typical Fe-based SMAs, exhibit significant fatigue [104]. Second, a high melting temperature inhibits diffusion processes from causing microstructural changes. Finally, because of the large number of loading cycles, the stresses utilized must be minimal. SMA fatigue characteristics might be enhanced by increasing the quantity of cold-working, annealing at lower temperatures, cycling at lower stresses and quicker rates [113]. The fatigue impact can also be reduced by thermomechanical training of the SMA specimen with pre-cycle loadings between (M_f) and (M_d) [114].

Throughout tension–compression loops, Wang and Zhu [115] investigated the cyclic behaviour of pseudoelastic SMA bars with buckling-restrained components. The SMA bars displayed satisfactory and stable flag-shaped hysteretic loops with minimal strength loss during cyclic tension–compression loadings. Moreover, the SMA bars displayed an exceptional self-centring capacity that is practically independent of strain rate.

Shi et al. [116] examined the impact of atmospheric temperature on SMA cable mechanical sensitivity and pseudoelastic fatigue behaviour. The SMA cable anchorage system and test setup details are shown in Fig. 5. They observed that the fatigue life of the SMA cable degrades with rising room temperature, and that the SMA cable fully terminated at the 699th iteration when the temperature range hit 60 °C.

3.3. Strain rate effects

The strain rate has a significant impact on the mechanical behaviour of SMAs. SMA transfers thermal energy as heat during forward phase transitions, whereas it absorbs energy through unloading [23]. During loading with high strain rates, SMA may not transfer thermal energy to the surroundings in a limited amount of time. As a result, the temperature of the material rises, altering the geometry of the hysteresis loops and transformation stresses [117]. Because the SMA utilized in structural response applications would be subjected to dynamic loadings, it is necessary to examine the effect of strain rate on the SMA prior to deployment.

Several studies have been conducted to examine the influence of loading strain rates on the behaviour and mechanical characteristics of SMAs. According to Liu and Van Humbeeck [93], the damping capability of the Ni–Ti SMA increased as the strain rate increased. Other experiments, however, have found that increasing the loading rate leads to a reduction in hysteresis and energy dissipation of the SMAs [97,118]. It was also discovered that increasing strain rates increases both forward and reverse transformation stresses [112]. Tobushi et al. [119] found that higher strain rates lowered the reverse transformation stress while increasing the forward transformation stress resulted in more energy dissipation. Soul et al. [120] discovered that for frequencies less than 0.05 Hz, the dissipated energy increases considerably, whereas for frequencies more than 0.053 Hz, it drops dramatically.

3.4. Temperature effects

Since shape memory transformations are a thermoelastic process that is affected by temperature as well as mechanical loads, the temperature is an essential variable that affects the shape memory behaviour of SMAs. The mechanical characteristics of SMAs are temperature dependent, which precludes many possible seismic applications and may restrict their performance in locations with wide temperature variations.

It has been observed that increasing the temperature causes a rise in transformation stress, therefore a lower stress magnitude is necessary to initiate the transformation. In other words, SME can be observed in an SMA at low temperatures, but a pseudoelasticity effect can be observed in the same SMA at high temperatures [17]. As indicated in Table 2, the composition of the alloy's components can influence the transition temperatures. However, in the pseudoelastic region, temperature change has little effect on initial stiffness and residual strain [23].

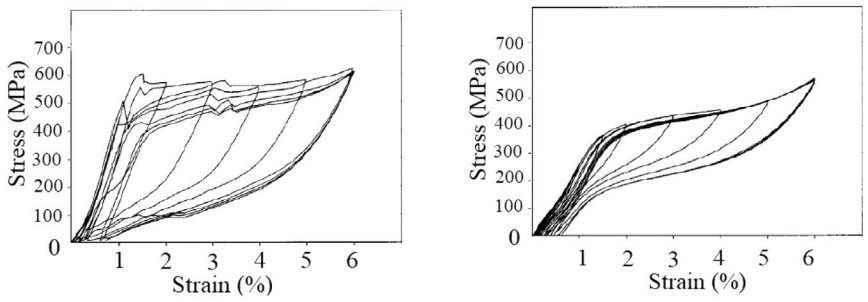

Fig. 4. Stress–strain curves of Ni–Ti subjected to quasi-static cyclic loading [112]: (a) 1.8 mm diameter Ni–Ti wire; (b) 25.4 mm diameter Ni–Ti bar.

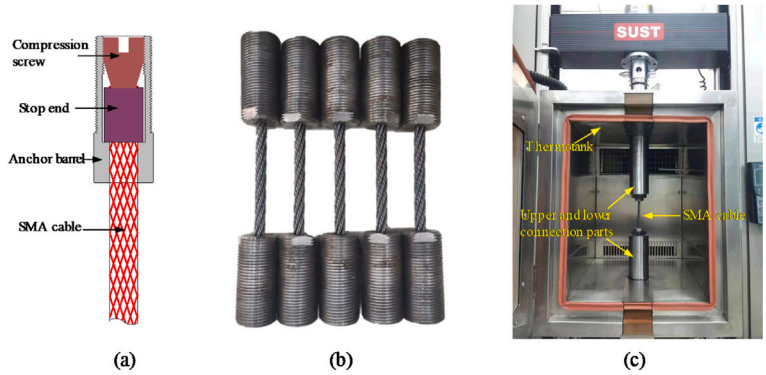

Fig. 5. (a) SMA cable anchorage system; (b) SMA cable specimens; and (c) test setup [116].

Table 2
Ni–Ti alloy compositions and transformation temperatures [121].

Composition (%)		Transformation temperatures (°C)			
Ni	Ti	M_f	M_s	A_s	A_f
49.1	50.9	−115.8	−30.7	1.9	44.6
49.5	50.5	−77.8	−18.5	9.0	53.0
50.0	50.0	−28.0	37.5	48.2	77.8

3.5. Re-centring

The capacity of a material to regain its initial geometry at multiple points during excitation prevents the structure from accumulating inelastic deformations [122]. Conventional civil engineering structures use a linear-elastic supplementary moment frame as a preserving force to decrease residual drifts in buckling restricted structures without full re-centring [123]. When external forces are eliminated, self-centring materials may reduce residual drifts through a nonlinear elastic stabilizing force [124]. According to Skinner et al. [125], contemporary design standards regard re-centring capacity to be a basic requirement for seismic isolation systems. Following factors exhibit insufficient re-centring capability [126]:

- significant residual displacements after an earthquake;
- displacement accumulation caused by the following earthquakes;
- increased maximum and residual displacements in seismic events with directivity effects.

Austenite SMAs possess the re-centring ability, but their dissipation capacity is relatively poor (particularly at higher loadings), and their behaviour may be described as nearly elastic. The re-centring capacity is independent of the element dimensions and unaffected by the strain rate of the loading [17]. The magnitude of the residual displacement in a nonlinear system can be greatly impacted by the form of the hysteresis loop [127]. The residual displacement averaged more than 40% of the peak displacements in several elastoplastic systems, with significant dispersion [128].

3.6. Corrosion and ageing

The corrosion resistance of Ni–Ti alloys is superior to most of SMAs due to the existence of a passive film that acts as a protective layer [129]. Nickel leakage can be minimized by changing Ni–Ti compositions (by partial substitution of Ti with Cu, Ag, Nb, Zr, Mo, and Ta) and improving its corrosion resistance [130,131].

In H_2SO_4 solutions, Fe–Mn–Si–Cr–I SMA with 8.8–12.80 wt% Cr exhibits comparable or superior corrosion resistance than stainless steel, although containing less Cr, since iron-based SMAs contain a colossal quantity of Si [132,133]. They are also impervious to intergranular erosion due to their high silicon concentration. The corrosion behaviour and mechanism of Fe–Mn–Si SMAs in Na–Cl solution, on the other hand, are not fully understood. The addition of Cu or La, as well as a very small amount of Ce, appears to increase corrosion resistance in Na–Cl solutions [134,135]. Some characteristics and procedures that can have a considerable impact on the corrosion resistance of these SMAs are listed below [136]:

- corrosion protection is reduced by increasing Mn and lowering Cr in the mixtures;
- additional Ni, N, and V in the mixtures improves the corrosion protection;
- although training diminishes corrosion protection, cold rolling reduces corrosion stability of the alloys, resulting in increased corrosion current and further recovery, whereas heating decreases corrosion resistance.

Cu-based SMAs have relatively low corrosion resistance; nevertheless, studies have shown that there are various approaches to increase the corrosion resistance of Cu-based SMAs, including additional compositions such as Al and Br, as well as polymer coating [137].

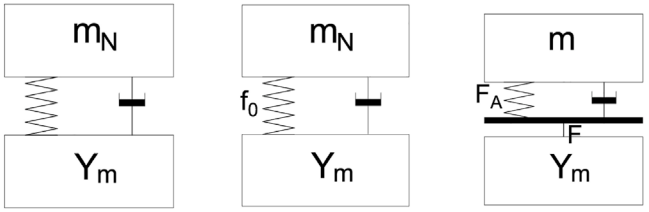

Fig. 6. Schematic concept of different vibration control concepts; (a) passive system; (b) semi-active system; (c) active system.

The ageing method can have an impact on the alloy's transition temperatures, thermal hysteresis, and mechanical characteristics [138]. The ageing of Cu-based alloys in the martensite or coexistence phase causes martensite stabilization, which raises the transformation temperature due to consecutive martensitic transition and precipitate production [139,140]. Ageing also has a substantial impact on the internal friction characteristics of Cu-based alloys, reducing damping capacity [140].

3.7. Grain size effects

The pseudoelastic behaviour of SMAs is significantly influenced by grain size, shape, and crystallographic orientation. Cu-based SMAs have higher grain sizes than Ni–Ti alloys. On the one hand, elastic stress concentrations in Ni–Ti SMAs are easily relieved by plastic deformation on grain boundaries. As a result, grain size and orientation have only a little impact on the mechanical behaviour of Ni–Ti SMAs, and high grain size is not necessary to achieve pseudoelastic behaviour [141]. Due to stress concentrations on grain boundaries, larger grains produce intergranular brittle fractures in Cu-basis SMAs.

In Fe-based SMAs, bigger grain size alloys exhibit superior shape memory effect behaviour since grain refinement reduces the suppressing of plastic deformation [142].

4. Basics of seismic response control

Structural control systems are used to decrease structural movements caused by a variety of dynamic loadings such as winds and earthquakes. Several vibration control devices have been implemented to enhance structural seismic response. These systems were primarily designed based on the structural materials' energy dissipation and absorption capabilities. As illustrated in Fig. 6, there are three primary seismic vibration control systems: passive, active and semi-active vibration control. In this figure, m_N signifies the neutralizer mass, Y_m reflects the mechanical mobility of the vibrating host structure, and F_A defines the internal actuation force.

In an Active Vibration Control (AVC), actuators that apply forces on object structures are controlled by an external power source. As a result, the massive quantity of electricity required for seismic control limits its application. Active mass dampers, hybrid mass dampers, and tendon controls are examples of AVC-based devices [143,144].

There is no need for an external power source in the Passive Vibration Control (PVC) device, and the impact forces are generated in response to structural movement. Viscoelastic solid and fluid dampers, friction dampers, and tunable mass dampers are examples of PVC-based devices [145,146]. The system, on the other hand, has difficulty adapting to changes in the structure. Semi-active control systems utilize a lot less energy than AVC-based devices to manage structural characteristics.

Semi-Active Vibration Control (SAVC) devices, which combine the best qualities of both passive and active control systems, are considered to be sufficient among these systems. As a result, they demonstrate a superior system capable of controlling the dynamic reaction of civil engineering structures [147]. SAVC-based devices include electro-rheological dampers, hydraulic dampers, variable orifice dampers, smart tuned mass dampers, and variable friction dampers.

5. Shape memory alloy modelling for seismic applications

So far, numerous researchers have focused on the martensitic phase change and presented constitutive models to characterize the extremely complicated behaviour of shape-memory materials. These models were created at either the microscopic or macroscopic levels. At the microscopic level, continuum mechanics use a slight quantity of material to create a relationship between deformation, strain, and stress at specified locations. Macroscopic level models, on the other hand, are intended to describe the SMA responses through a phenomenological approach. Some of these models are heavily reliant on thermodynamic principles, whilst others are constructed by fitting material parameters with experimental data. Herein, a brief breakdown of the existing models is provided:

- phenomenological macroscopic constitutive models on the basis of stress, strain, and temperature, with postulated phase change kinematics supplied by simple mathematical expressions proposed by Tanaka [13], Liang and Rogers [148], Brinson [149], Boyd and Lagoudas [150,151], Li et al. [152], Tobushi et al. [153] and Sun and Rajpakse [154].
- Devonshire's hypothesis-based one-dimensional polynomial computational models with an expected polynomial-free energy potential, permitting PE and SME characterization, presented by Falk et al. [155,156].
- free energy and dissipation potential thermodynamic models developed by Patoor et al. [157], Sun and Hwang [158,159], Huang and Brinson [160], and Boyd and Lagoudas [161].
- plastic flow models based on solid-state physics dislocation theories proposed by Graesser and Cozzarelli [20,21], which was later improved by Wilde et al. [162], Zhang and Zhu [163], and Ren et al. [164].

In the following sections, we focus on discussions of three of the most frequently utilized one-dimensional SMA material models for seismic design purposes.

5.1. Graesser and Cozzarelli's model

One of the initial fundamental numerical models for the hysteretic stress–strain behaviour of SMAs was developed by Graesser and Cozzarelli [20,21]. The concept is an extended form of Wen [165] and Ozdemir's [166] strain rate-independent material hysteresis hypotheses. The initial Ozdemir model is rate-dependent, however, Graesser and Cozzarelli established that the stress–strain correlations are rate-independent. The formula is as follows:

$$\dot{\sigma} = E\left[\dot{\varepsilon} - |\dot{\varepsilon}|\left(\frac{\sigma-\beta}{Y}\right)^{n}\right] \tag{3}$$

where σ is one-dimensional current stress, E is the austenite phase's elastic modulus (Initial elastic modulus), Y is the yield stress at (M_s), and n is a constant controlling the sharpness of the transition from elastic state to phase transformation; $\dot{\sigma}$ and $\dot{\varepsilon}$ are the time derivatives of stress and strain, respectively. β is one-dimensional back stress, and it is calculated as follows:

$$\beta = E\alpha\left\{\varepsilon_{in} + f_T|\varepsilon|^{c} erf(a\varepsilon)\,[u(-\varepsilon\dot{\varepsilon})]\right\} \tag{4}$$

where f_T, a, and c are material constants that determine the type and magnitude of hysteresis, the amount of elastic recovery during unloading, and the slope of the unloading stress plateau, respectively. When f_T=0, the model is completely martensitic, but when f_T>0, the

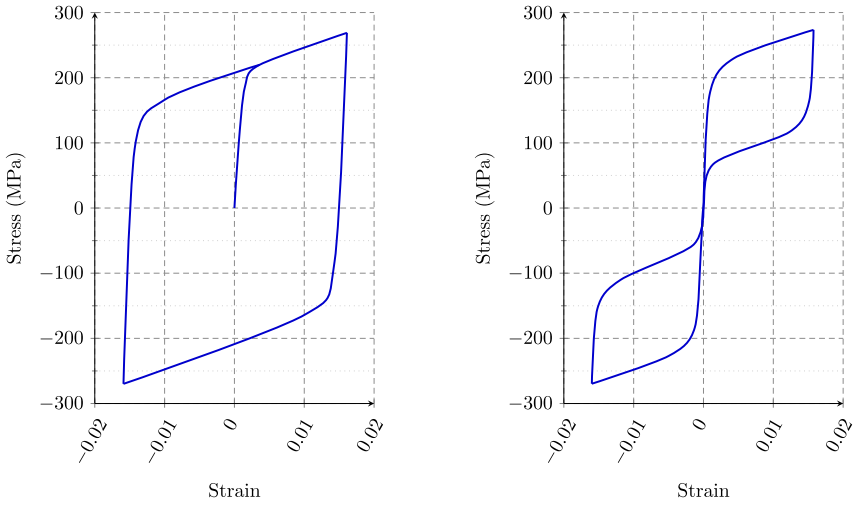

Fig. 7. Schematic stress–strain curves of SMAs (model parameters: $\varepsilon = 0.016\sin(t)$, $Y = 210$ MPa, $E = 28,500$ MPa, $\alpha = 0.0197$, $n = 3$, $a = 2,500$, $c = 0.001$, $f_T = 0.0$): (a) twinning hysteresis ($T < M_f$); (b) pseudoelasticity ($T > A_f$) [20,21].

model displays pseudoelasticity behaviour. α is a constant that governs the slope of the stress–strain curve in the inelastic range, and it is denoted as:

$$\alpha = \frac{E_Y}{E - E_Y} \tag{5}$$

where E_Y in the inelastic range is the slope of the stress curve (after yielding).

ε_{in} is the inelastic strain, given by:

$$\varepsilon_{in} = \varepsilon - \frac{\sigma}{E} \tag{6}$$

The error function is defined as:

$$erf(x) = \frac{2}{\sqrt{\pi}} \int_0^{\pi} e^{-t^2} dt \tag{7}$$

Eq. (7) is a straightforward expression to model the return of the $\sigma - \varepsilon$ curve during unloading so that with an appropriate selection of f_T, a and c the inelastic stress is fully recovered at α=0.

The unit step function is defined as:

$$u(x) = \begin{cases} +1 & x \geq 0 \\ 0 & x < 0 \end{cases} \tag{8}$$

where equation (8) will activate the last term in Eq. (4) just during unloading.

The simplicity of Graesser and Cozzarelli's model allows to encompass both the pseudoelastic effect and the martensitic hysteresis with its sub-loops due to discontinuous transformation cycles. However, this model does not account for post-transformation martensitic hardening at large stresses, which is essential in seismic applications. As a result, to overcome the aforementioned restriction, this model requires further improvements.

The material constants E, Y, and α are chosen for the sake of model demonstration to be 200,000 MPa, 210 MPa, and 0.0197, respectively. Furthermore, the over-stress power is set to $n = 3$, and the starting constant f_T is set to zero. A strain-controlled test with a sinusoidal cyclic loading condition ranges from −0.016 to 0.016. The results are depicted in Fig. 7.

5.2. Wilde, Gardoni and Fujino's model

Wilde et al. [162] improved the Graesser and Cozzarelli model by simulating a uniform transition between the elastic and pseudoelastic plateaus to reflect the potential of characterizing material behaviour following phase transformation martensitic hardening. This impact is included in the model in the second line of Eq. (3), which is given by:

$$\begin{aligned} \dot{\sigma} =& E \cdot \left[\dot{\varepsilon} - |\dot{\varepsilon}| \cdot \left(\frac{\alpha - \beta}{Y}\right)^n\right] \cdot u_1(\varepsilon) + E_m \cdot \dot{\varepsilon} \cdot u_{II}(\varepsilon) + \\ & (3 \cdot a_1 \cdot \dot{\varepsilon} \cdot \varepsilon^2 + 2 \cdot a_2 \cdot sgn(\varepsilon) \cdot \dot{\varepsilon} \cdot \varepsilon + a_3 \cdot \dot{\varepsilon}) u_{III}(\varepsilon) \end{aligned} \tag{9}$$

where the unit step functions are defined as:

$$u_I(\varepsilon) = (1 - u_{II}(\varepsilon) - u_{III}(\varepsilon)) \tag{10}$$

$$u_{II}(\varepsilon) = \begin{bmatrix} 1 & |\varepsilon| \geq \varepsilon_m \\ 0 & otherwise \end{bmatrix} \tag{11}$$

$$u_{III}(\varepsilon) = \begin{bmatrix} 1 & \varepsilon.\dot{\varepsilon} > 0 \quad and \quad \varepsilon_1 < |\varepsilon| < \varepsilon_m \\ 0 & otherwise \end{bmatrix} \tag{12}$$

where ε_1 represents the strain at (M_s) and ε_m represents the strain at (M_f). The second term, which involves E_m, simulates the elastic behaviour of martensite and is non-zero only when $\varepsilon > \varepsilon_m$. The last term governs the transition from slope E_Y to slope E_m and is non-zero only when the total strain (ε) is inside the (ε_1, ε_m) transition zone during loading. The smoothness of the transition is controlled by the constants a_1, a_2, and a_3. Although the model can characterize the hysteresis loops at a particular strain rate and temperature with exact numerical values of the constants, the model is still rate–temperature independent. The adjustment of gradient at strain ε_2 determines the smoothness of the transformation (Fig. 8).

5.3. Tanaka's model

In static tensile testing, an SMA wire may expel internal heat created during the loading phase while absorbing heat from its surroundings during the unloading phase. While isothermal circumstances may be used for static testing, as the strain rate increases, the system behaviour becomes more adiabatic [167]. As a result, a dynamic model must incorporate the mechanical and kinetic principles that determine the material's martensitic fraction. Tanaka's model [13] is a temperature-dependent phenomenological model that takes into account crystallographic structural changes via an internal state shift, the martensite percentage, ξ, which characterizes the range of the transformation. The model may be analytically written as follows:

$$\begin{aligned} \dot{\sigma} = E\dot{\varepsilon} + \Theta\dot{T} + \Omega\dot{\xi} \quad with \quad E = E_A + (E_M - E_A)\xi \\ and \quad \Theta = \Theta_A + (\Theta_M - \Theta_A)\xi \end{aligned} \tag{13}$$

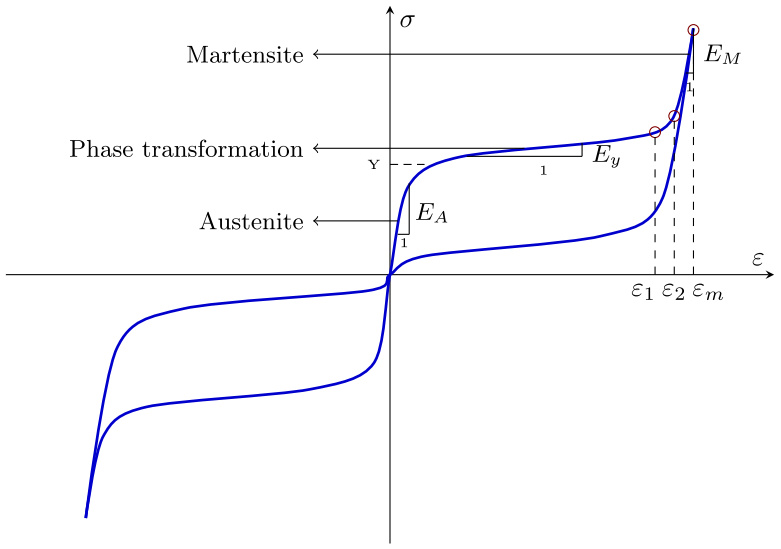

Fig. 8. Schematic stress–strain relations of the extended hysteretic model of SMA [162].

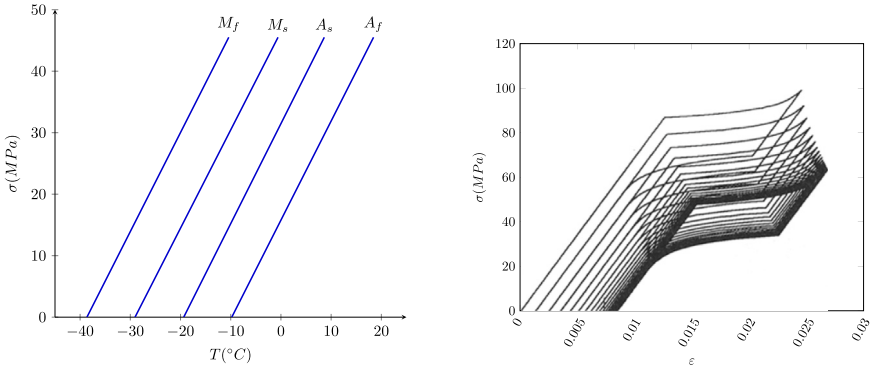

(a) (b)

Fig. 9. Schematic stress–strain curves of SMAs (model parameters: E = 7000 MPa, Ω = −700, and Θ = −700): (a) transformation lines; (b) stress–strain hysteresis during cyclic isothermal loading [13].

where σ denotes normal stress, T temperature, ε strain, Ω phase transformation tensor, E elastic modulus, and Θ thermoelasticity modulus. Pure austenitic and martensitic phases are denoted by the subscripts A and M, respectively.

The stress–strain hysteresis in a SMA at$T = 30\ ^\circ C$ under cyclic loading between 0 and 120 MPa, which encloses the martensitic/reverse transformation regions, is depicted in Fig. 9.

6. Shape memory alloys seismic applications for civil engineering structures

SMAs have been used in many different applications in buildings such as base isolation, bracing, cables and etc. thanks to their excellent properties. In this part, we attempted to trace the historical development while also introducing the most recent advances and novel structural response control methods in SMA seismic applications.

6.1. SMA-based passive vibration control

The pseudoelastic behaviour of SMAs is employed in the PVC system. It uses damping and re-centring features to decrease the responses and deformations of a structure subjected to extreme loading conditions. SMA-based PVC applications can be divided into two major groups: base isolation and energy dissipating devices.

SMA-based isolators positioned between a superstructure and substructure in a base isolation system are developed for an uncoupled system that limits the transfer of seismic input energy from the ground movement to the superstructure. On the other hand, SMA components included a system for energy dissipation that absorb vibrational energy based on the hysteretic stress–strain relationship. SMA-based PVC devices offer a higher damping capability in the martensite phase but external heating is required in their activation procedures. Pseudoelastic SMAs, on the other hand, have a smaller damping capacity but can re-centre the structure with low residual stress.

6.1.1. Base isolation devices

The original objective of seismic isolation dampers is to limit the influence of induced seismic forces on the structure throughout an earthquake. As a result of the decrease of earthquake excitation and deformations in the structure, the structure's integrity is preserved [22].

The structures with SMA-based isolation devices generally consist of three components; super-structure, sub-structure and the isolator. In buildings, they are mainly installed between the foundation and first suspended level [168]. Experimental studies have shown that SMAs are feasible and suitable candidates for isolation devices based on their excellent properties such as high damping capacity and re-centring capability as mentioned before [27,169]. Especially when an ideal isolator is expected to exhibit variable stiffness according to the base

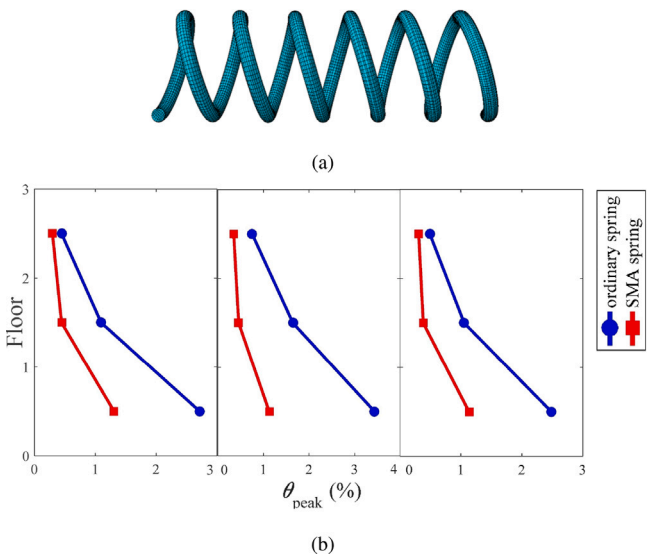

Fig. 10. (a) Proposed model; (b) peak interstorey drift ratio of the superstructure under three different earthquake motions [170].

excitation, in these cases SMAs simply excel because of their intrinsic damping mechanism provided by phase transformation [168].

Liu et al. [170] investigated the seismic behaviour of a pseudoelastic SMA spring in multi-storey steel frame isolators (Fig. 10a). Their findings showed that the SMA spring has effective self-centring and damping capabilities, with an equivalent damping ratio of more than 2%. In comparison to regular elastic springs, their SMA spring allowed exceptional control of the superstructure's peak and residual deformations.

Fig. 10b shows that, for all studied seismic activities, the peak interstorey drift proportions tend to concentrate at the first storey, but the deformation concentration degree is greatly decreased by utilizing SMA springs. SMA springs outperform conventional springs in terms of deformation control over the entire building height.

Wang et al. [171] proposed a novel pseudoelastic SMA self-centring seismic base isolator in U-shaped dampers (SMA-UDs). They investigated two different designs, which incorporate the SMA-UDs into a conventional laminated rubber bearing with a lead core or with steel-UDs. Their findings have shown that the proposed base isolation system exhibits superior self-centring, adequate energy dissipation, stable and satisfactory flag-shaped hysteresis loops, a significant reduction in residual deformation under cyclic loading and ease of inspection and repair after a severe earthquake.

The effective damping ratios of the self-reentering base isolators (SMA-LRBs and SMA-SRBs) rose somewhat with incremental displacement, but the values progressively stabilized between 14.2% and 18.1% for high displacement amplitudes. This property verified the beneficial effect of the lead core or steel-UDs in improving the energy dissipation of the SC base isolators.

Dezfuli and Alam [172] developed the novel SMA-based Lead Rubber Bearing (LRB) by laying ferrous SMA wires across the LRB in an asymmetrical double crossing arrangement (Fig. 11a). When compared to typical LRBs, the proposed SMA-LRB exhibited a significantly lower shear strain demand (up to 46% lower) and greater energy absorption (up to 31% higher). Furthermore, the pseudoelastic impact of Fe-based SMA (above 13% strain) increases LRB re-centring performance by lowering residual displacement by approximately to 33% [173]. Pre-straining SMA wires, which is required in the method of installing wires on elastomeric vibration dampeners, may increase SMA-LRB performance by improving its recentring characteristic. For example, 3% pre-strained SMA wires might minimize residual deformation of SMA-LRB by 19%.

Table 3
Based on the experimental results, a comparison of steel-based and SMA-based bracing systems is made [177].

Properties	Type of bracing frame	
	Steel-based	SMA-based
In-plane frequency (Hz)	35	35
Out-of-plane frequency (Hz)	39	46.8
Damping ratio (%)	1.3	1.0
Theoretical stiffness (kN/mm)	9.5	17.6
Experimental stiffness (kN/mm)	2.05	15.4

Dezfuli et al. [174] suggested a novel modelling approach of SMA-wire based rubber bearings in another work, and the dynamic performance of a three-span continuous concrete-girder highway bridge structure was evaluated under near- and far-fault motions (Fig. 11b). The results reveal that SMA wires may sufficiently minimize shear strain demand in LRBs and restrict deck movement by enhancing the effective stiffness of the elastomeric isolator. As a consequence, the likelihood of bearing failure and unseating on the deck may be significantly reduced. Furthermore, owing to SMA-LRBs' increased energy absorption capabilities, such innovative bearings may greatly enhance the seismic behaviour of bridges in terms of base shear.

Habieb et al. [176] investigated hybrid seismic base isolation of a historical masonry church by Unbonded Fibre Reinforced Elastomeric Isolators (UFREI) and SMA wires as shown in Fig. 12. It was observed that the utilization of SMA wires with a particular pre-strain considerably improve the energy dissipation capacity of the base isolation system and reduces the horizontal displacements of the masonry church. The suggested configuration with a 2% pre-strain SMA wire model displays the biggest decline of the church's diagonal deformation and significantly decreases damage (from demolition to mild damage level) in the case of strong seismic events due to its high energy absorption capacity.

6.1.2. Energy dissipation devices

Varughese and El-Hacha [177] investigated two steel lateral resistance frames, one with steel yielding fuse and the other with Nitinol yielding fuse (Fig. 13). The analysis indicates that the stiffness of the stiffeners has no effect on the natural frequency of the structural system, but that the system's connection to the rigid floor alters the natural behaviour. Furthermore, both frames have the same natural frequency in-plane (Table 3). This suggests that the anchorage at the columns, rather than the stiffness of the constrained elements, dominates the stiffness of the system.

Kamgar et al. [178] inserted SMA fibres in two directions in a steel shear wall (SSW) (Fig. 14). The findings demonstrated that the buckling load increases and that the SME behaviour regulates the total out-of-plane displacement of the SSW and nonstructural deterioration.

Wang et al. [179] employed SMA bolts in two distinct column-foundation connections, one with and one without pre-tensioning (Fig. 15). The results showed remarkable hysteresis, as well as good self-centring and high energy dissipation. Another advantage of this method is that the bolts can continue to function efficiently even after severe earthquakes without needing to be replaced.

Fig. 16 demonstrates the pseudoelastic SMA-based retrofitting device proposed by Cardone et al. [180] to improve the mechanical properties of steel joints in heritage structures. Testing results revealed that the presented mechanism was viable in reducing temperature-induced stress differences 80%–90%.

Other researchers investigated the improvement of the self-centring ability of the structures throughout the application of SMAs. Wang et al. [100] discussed the mechanical performance of a novel self-centring damper equipped with a group of kernel elements (SMA ring springs). The results indicated that the system demonstrated anticipated mechanical behaviour with a satisfactory stable flag-shaped hysteretic response without any fracture. Additionally, the damper

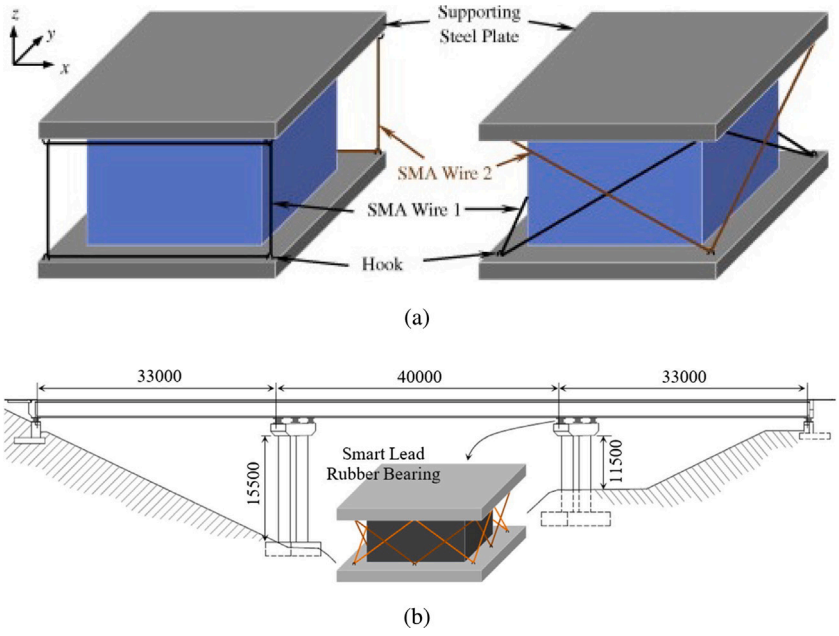

Fig. 11. SMA wire-based lead rubber bearing: (a) smart rubber bearing with straight and crossing SMA wires; (b) wire-based SMA-LRB isolator for a multi-span bridge (dimensions are in mm) [172,174,175].

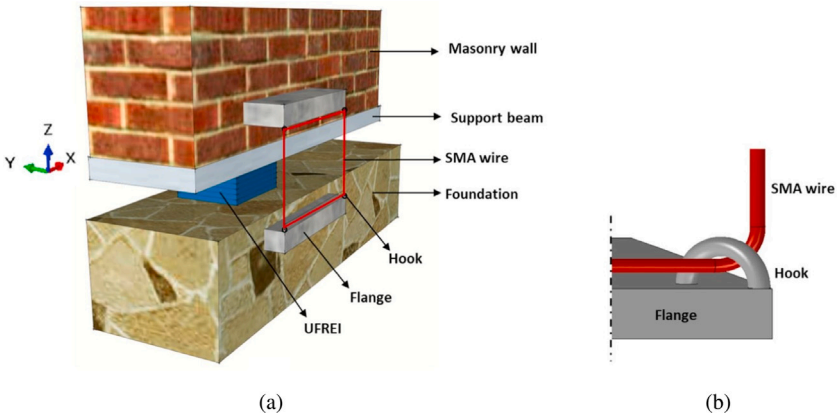

Fig. 12. The schematic of the proposed system and SMA strand in the isolation system of masonry constructions; (a) schematic of the installation; (b) configuration of the hook [176].

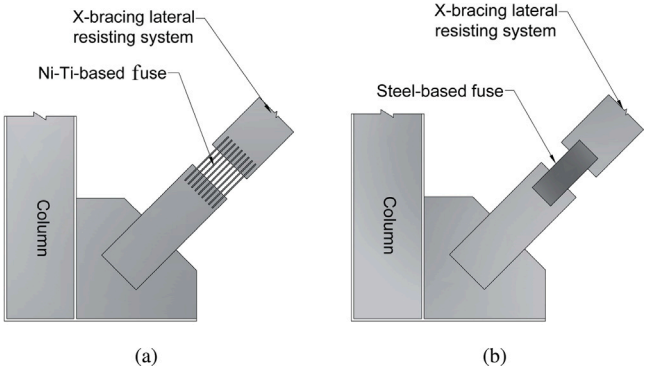

Fig. 13. (a) Bracing frame with SMA-based yielding fuse; (b) bracing frame with steel-based yielding fuse [177].

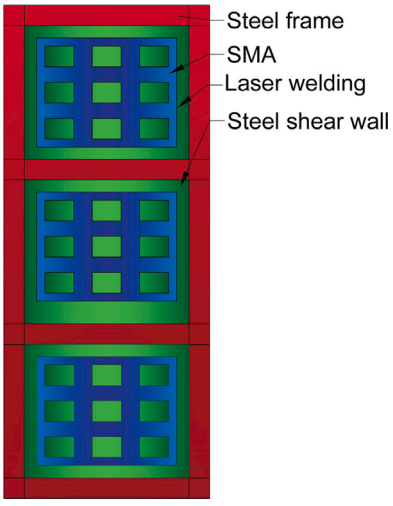

Fig. 14. The steel frame retrofitted with steel shear walls and SMA fibres strips [178].

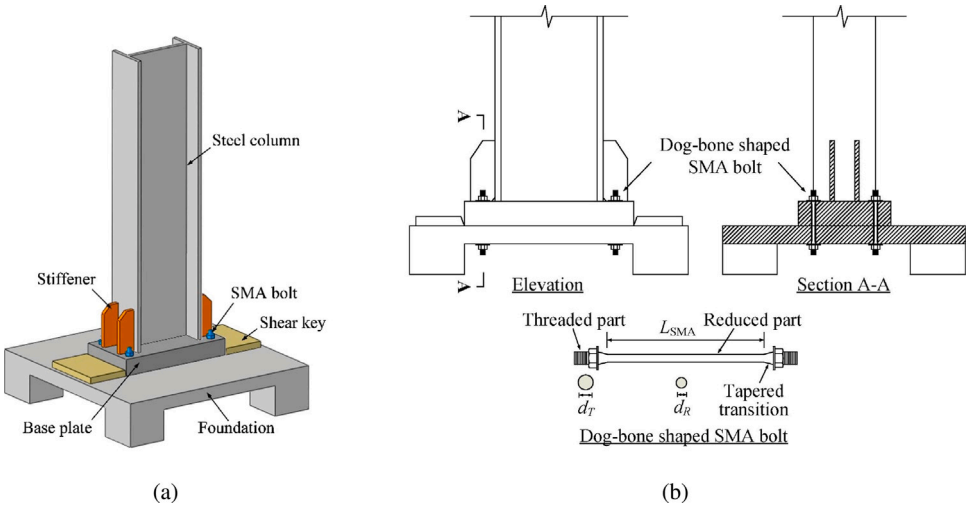

Fig. 15. Schematic of steel column and foundation connection with SMA bolts; (a) configuration; (b) cross sections [179].

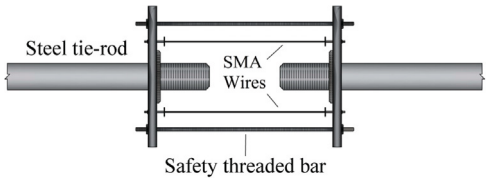

Fig. 16. Schematic of the proposed SMA-based system [180].

specimen exhibited excellently self-centring capability with no residual displacement and good energy dissipation capacity with an EVD up to 18.5%.

Dong et al. [181] analysed the seismic responses of the steel frame with self-centring energy dissipation braced on the shape memory alloy cables (SMA-SCEB). The numerical results demonstrated that the self-centring energy dissipation brace can considerably reduce the residual drift ratio of the structure with lower peak acceleration.

Wang and Zhu [182] also investigated the application of SMA bars in the self-centring reinforced concrete wall. The model displayed excellent self-centring and satisfactory energy dissipation capacity with almost no residual deformation after loading cycles with a peak drift of 2.5%.

SMAs also can be used to enhance the performance of bracing frames. Mirzai and Attarnejad [183] proposed a Re-centring Damping Device (RDD) including an Eccentrically Braced Frame (EBF) equipped with SMA that performs as a rapid repair fuse. Their results illustrated that the proposed RDD could reduce the maximum inter-storey drift ratio and the residual drift by 57% and 86.99%, respectively.

As demonstrated in Fig. 17, Mahmoudi et al. [184] examined the structural property of different frames equipped with SMA bars X-knee-braced frames (X-KBFs). The results demonstrated that the SMA-KBFs, significantly reduces the permanent roof displacements, resulting in a considerable increase in the re-centring capacity of the structures.

The near-surfaced-mounted (NSM) technique is another innovative method that can address issues such as growing fractures and crack breadth caused by yielding loads and lowering deflection in RC beams at mid-span. This approach was used by reinforcing the structure using FRP. According to the research, the RC beam reinforced by the pre-stressed Fe-SMA NSM method has a very modest enhancement in ultimate loads. In contrast to the RC beams strengthened by the pre-stressed FRP NSM technology, the pre-stressed Fe-SMA NSM approach does not reduce the ductility of the retrofitted RC beams by applying a pre-stressing force to the concrete [185].

Abbas et al. [186] investigated the application of the NSM technique for RC bridge columns by using five different types of NSM-SMA bars with FRP layers as illustrated in Fig. 18.

It was discovered that columns rehabilitated using NSM-FeNCATB could sustain more deformations than other repaired columns, resulting in the greatest deformed flexibility among other columns. This is due to the FeNCATB alloy having the highest strain threshold and post-yield stiffness of any alloy. They also found that repaired columns using NSM-FeMnSi bars and FRP coverings absorbed more energy than other rehabilitated columns. It was also revealed that the more self-centeredness, the lower the damping ratio produced. This is owing to the pseudoelastic structure of the NSM-SMA bars.

Ke et al. [187] designed a performance-spectra-based approach for evaluating the earthquake resistance of commercial steel frames using SMAs with the connection detail shown in Fig. 19, while taking into account multi-performance characteristics and hysteresis transformation. They noted that the nonlinear response characteristics of a steel frame with SMAs are susceptible to vibrant and hysteretic properties when various yielding stages are considered, and considerable customization may be accomplished by modifying model properties.

Chen et al. [188] studied the use of a SMA-based damper (Fig. 20) in the dynamic response of a wind-loaded tower-line. They discovered that as damper stiffness was increased, the maximum responses steadily decreased. The ideal self-centring values for maximum dislocation, velocity, and acceleration in in-plane vibration are 1.0, 2.0, and 1.0, respectively, and for out-of-plane vibration are 1.0, 1.0, and 0.8, respectively. Furthermore, it was shown that the impact of operating temperatures on maximum damper displacement is substantially lower than the impact of damper stiffness.

6.2. SMA-based active vibration control

The active control technique makes use of SMAs' shape memory behaviour, due to their temperature-induced transition, they can be used as actuators in active or shape control systems. When heated, they may generate enormous forces by recovering their original undeformed configuration. For instance, controlling the pseudoelastic stress–strain curve of thin SMA wires by resistance heating and forced convection cooling for temperature control [189]. Another group of concepts includes additional SMAs besides typical damper elements based on their ability to bring on forces and adaptive stiffness [99].

Rogers [190] performed several experimental studies on the dynamic behaviour and control of structural vibration by SMAs as a distributed (integrated) strain sensor and a transient vibration actuator. It is noted that an SMA composite structure might be a suitable material

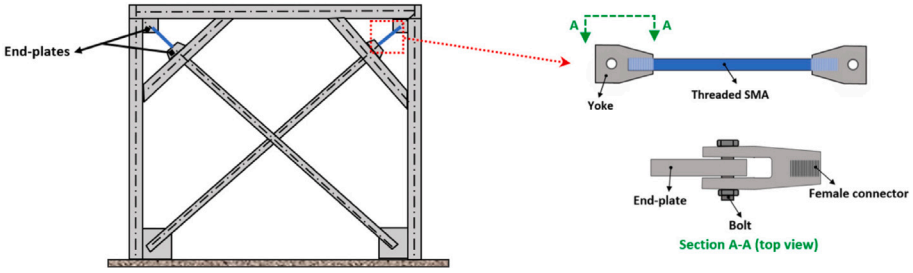

Fig. 17. X-KBFs equipped with SMA-based bars [184].

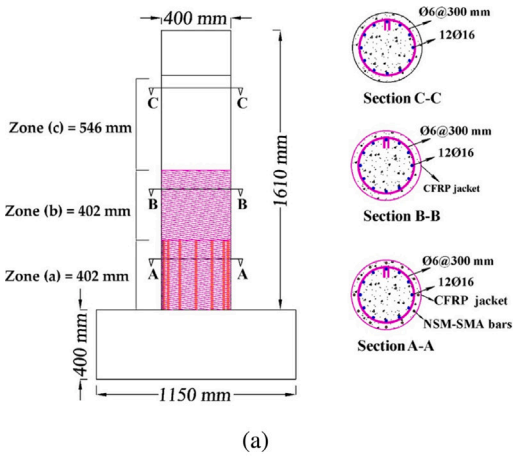

Fig. 18. Schematic of the proposed NSM-SMA retrofitting methods; (a) circular cross-section column; (b) rectangular cross-section column [186].

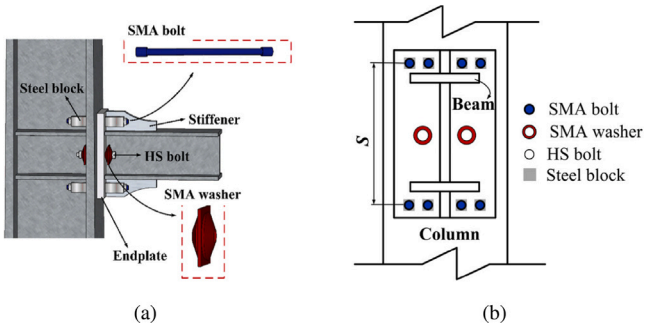

Fig. 19. SMA connector: (a) setup and (b) a sample measurement in a three-storey system [187].

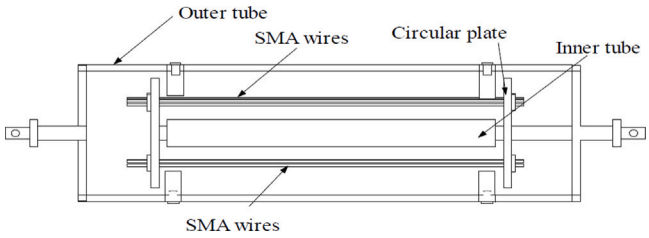

Fig. 20. Schematics of the proposed SMA-based damping system [188].

providing uniform dynamic response over a large temperature range or give some other favourable dynamic response as a function of temperature.

Chen and Levy [191] proposed a mathematical model of active vibration control of a flexible beam cover with SMA layers. It was noted that modifying the elasticity modulus and temperature of the SMA element affects the natural frequency of the beam. Also for active vibration control, the response amplitude and vibration time depend on many factors such as the ratio of austenite to martensite elasticity modulus.

Shahin et al. [192] studied the application of two SMA wire tendons for vibration control which were attached in a criss-cross way in the one-mass one-bay model of frame. The authors reported that, under adequate control schemes, both the passive and active implementation of the SMA tendons would effectively reduce the relative displacement of the top floor mass and the base of the frame structure, with a greater effectiveness of the latter. Williams et al. [193] developed an adaptive tuned vibration absorber in the form of a mass-ended cantilever SMA spring with its stiffness tuned via resistance heating, which can be effectively use in passive vibration control applications. Further mass was performed as an adjustable damping system with a variable natural frequency. A set of multiple springs that were heated gradually were used to maintain a more inconsiderate or gradual variation in stiffness. This mechanism of multiple springs with adaptive stiffness can apply to the design of adaptive tuned mass dampers for civil engineering structures [99].

As one of the initial experiments related to SMA-based AVC devices, Baz et al. [194] conducted a numerical study to demonstrate the possibility of using Ni–Ti actuators as an AVC-based device in a flexible beam (see Fig. 21). The finite element method was used (Eq. (14)) to divide the flexible beam into n elements. Consider an element that has a Ni–Ti actuator attached to it as shown in Fig. 21.

The element's length is L_i and located between nodes i and j. The external forces and moments acting on nodes i and j referred as V_i, M_i, V_j and M_j, respectively. Based on the Bernoulli–Euler beam's theory, these forces are related to the linear and angular deflections of the element y_i and θ_i, and y_j and θ_j.

$$\begin{bmatrix} V_i \\ M_i + M_N \\ V_j \\ -M_j - M_N \end{bmatrix} = \frac{E_i I_i}{L_i^3} \begin{bmatrix} 12 & 6L_i & -12 & 6L_i \\ 6L_i & 4L_i^2 & -6L_i & 2L_i^2 \\ -12 & -6L_i & 12 & -6L_i \\ 6L_i & 2L_i^2 & -6L_i & 4L_i^2 \end{bmatrix} \begin{bmatrix} y_i \\ \theta_i \\ y_j \\ \theta_j \end{bmatrix} \tag{14}$$

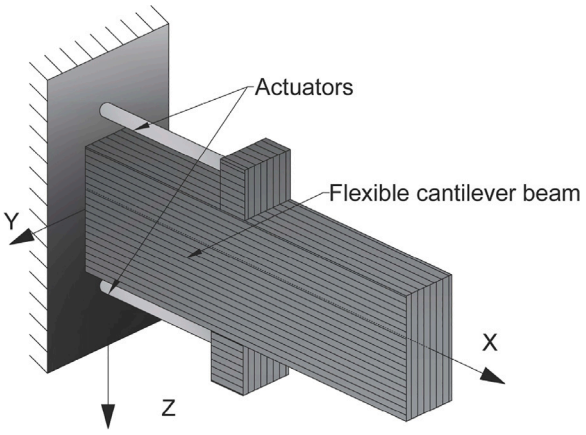

Fig. 21. Schematic of the active control system of a cantilever beam by SMA bars as actuators [194].

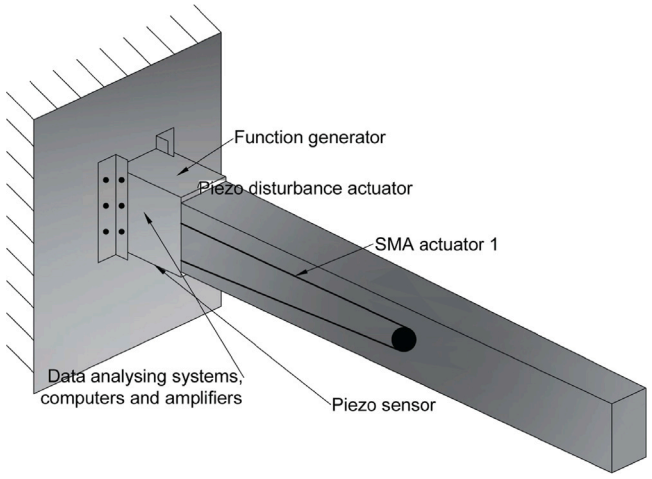

Fig. 22. Schematic of the experimental configuration [195].

where $E_i I_i = E_a I_a + E_b I_b$ is the flexural rigidity of the beam-actuator system, $E_{a,b}$ is Young's modulus of the actuator and beam respectively, $I_{a,b}$ is the moment of inertia of actuator and beam, respectively and M_N is the control moment generated by the Ni–Ti actuator.

The results revealed that after submitting the system with two triggered Ni–Ti bars to a load, the displacement begins to settle after 8 s, but in the uncontrolled system, there were somewhat unstable deformations even after 20 s. Furthermore, it has been claimed that efficient vibration control demands the use of two Ni–Ti actuators for each degree of freedom to be regulated. Finally, it is proposed that increasing the actuators' input power leads to effective damping of structural vibrations.

Vishal et al. [195] investigated the use of Ni–Ti wires as actuators for active vibration suppression in a piezoceramic laminated flexible cantilever beam with low natural frequency and closely spaced modes as seen in Fig. 22.

Vibration control was carried out experimentally at the beam's initial modal resonance frequency, where the magnitude of vibration is greatest. The actuation force was controlled using Matlab/Simulink and a data collecting system using the pulse width modulation method.

The testing results demonstrated a surprisingly high vibration suppression of about 95% and the ability to suppress vibrations of extremely high amplitude. The controller provided fully dissipated vibration energy in 5s as opposed to 60s that the system takes without control. Even when subjected to extremely huge abrupt shocks, the system remains stable.

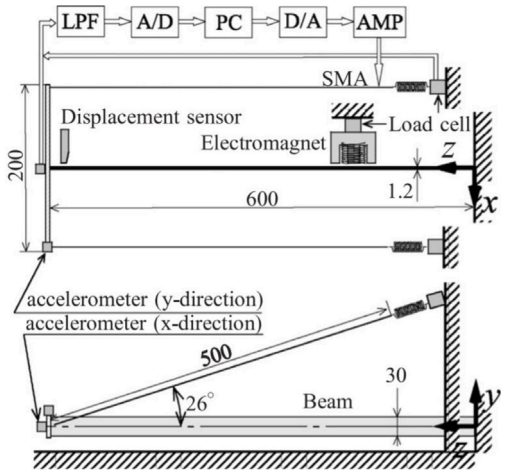

Fig. 23. Experimental configuration [196].

Suzuki and Kagawa [196] developed a control system that utilizes SMA actuators as tendons. SMA in a tendon mechanism is regulated in a push–pull way using H-infinity theory and accounting for actuator performance unpredictability (Fig. 23). Using this technique, the cantilever beam's four vibrational modes (three bendings and one torsional) may be damped at the same time.

They inserted SMAs diagonally in a beam–SMA structure to regulate the bending and torsional vibrational modes of a flexible beam, then measured and theoretically modelled the characteristics of an actuator comprising of an SMA and a spring. Table 4 shows the natural frequencies and modes of the cantilever computed using the finite element technique.

The SMA is energized by a voltage forcing it to contract and exert a phase-transformation force on the load cell. The proposed active controller systems significantly damped both bending and torsional vibrational modes.

Nakshatharan et al. [197] examined the application of Ni–Ti wires in an active vibration suppression of a piezoceramic laminated flexible cantilever beam, characterized by the low natural frequency with closely spaced modes. The test comprised of a beam with integrated sensor and actuators, electronics for sensor and actuators and, hardware and software for control processes. The controller device does not need a system model or any tuning parameters. The experimental result demonstrated a significant high vibration suppression of around 95%, with the ability to suppress a very high magnitude of vibration. Stable performance is achieved after around 9s and it can be robust even for an extreme sudden disturbance.

Alambeigi et al. [198] investigated the free and forced vibration behaviour of a sandwich beam with functionally graded porous core and composite face layers embedded with SMA. It was observed that increasing the sandwich beam temperature leads to an increasing in the structural stiffness and entering the austenite phase due to the SMA's temperature properties. Also, it was resulted that an increasing porosity coefficient leads to lower stiffness and mass and higher natural frequency.

6.3. SMA-based semi-active vibration control

The semi-active control technique makes use of the temperature-dependent increment in elasticity modulus. The elasticity modulus of SMAs in the austenite state is three times that of the martensite state. When heated, incorporated SMA components stiffen the superstructure, allowing the natural frequency of the structures to be actively adjusted.

Heinonen et al. [199] developed a semi-active device to reduce structural vibrations by altering the stiffness of the device that connects

Table 4
Calculated modes of x-translational degree of freedom at displacement sensor and electromagnet, rotational degree of freedom at cantilever end, and the natural frequencies, and assumed damping ratios of cantilever [196].

Variables	1st bending	2nd bending	1st torsional	3rd bending
Displacement sensor ($kg^{-0.5}$)	−1.67	−0.666	0	1.36
Electromagnet ($kg^{-0.5}$)	−0.0193	−0.198	0	−0.468
y-axis ($kg^{-0.5}m^{-1}$)	−4.7	24.6	0	−31.9
z-axis ($kg^{-0.5}m^{-1}$)	0	0	−51.6	0
Frequency (Hz)	1.1	11.3	13.2	30.3
Damping ratio	0.002	0.002	0.002	0.002

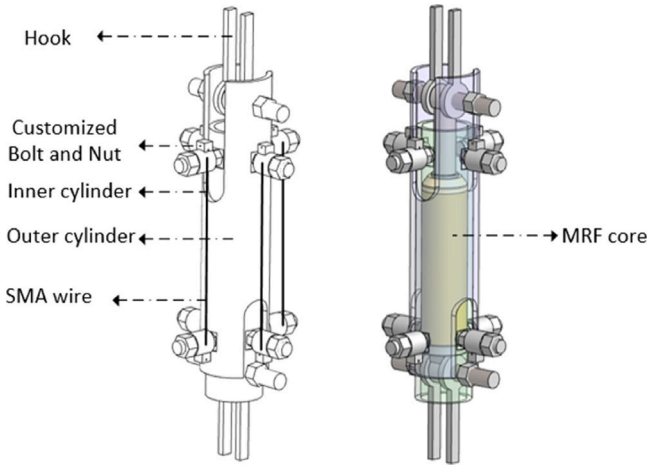

Fig. 24. Configuration of SMA-MRF-based structural control system [202,203].

the structure to the base. The functioning mode of the system was controlled by the SMA string temperature. Heating activated the stiff mode, on the other hand, cooling activated the soft mode. Both static and dynamic loading tests demonstrated that the control of boundary conditions can be applied to adjust the stiffness. The average stiffness ratio of each test set reached generally from 3.4 to 4.1, and the maximum stiffness ratio was 5.0.

Cismasiu and Santos [200] proposed a semi-active vibration control device based on SMA austenitic wires. The system controls the feedback measurements, as a result, it adjusts the strain in the SMA wires to improve its dynamical behaviour. The accumulated strain in the wires is a result of just the structural motions, without external energy input into the system. The system represented excellent dissipating energy capacity while keeping the SMA wires inside the recoverable range to minimize the rheological effects related to cumulative creep.

Mishra et al. [201] developed the convectional linear Tuned Mass Damper (TMD) by replacing the linear spring and viscous damper with an SMA spring. The system has shown excellent controlling behaviour and simultaneously reduction in the displacement of the system itself with eliminating almost all residual displacement.

Zareie and Zabihollah [202,203] established a semi-active control element based on the combination of Magneto-Rheological Fluid (MRF) and pseudoelasticity effect of SMA to dissipate a considerable amount of energy in marine structures (Fig. 24). They studied earthquakes occurring near the coast that were selected as examples of typical non-deterministic stimulation applied to the structure. These three earthquakes were Christchurch (NZ), Darfield (NZ) and Parkfield (USA) with M_W values of 6.2, 7 and 6, respectively.

The SMA-MRF element is shown to minimize the maximum displacement of the first storey for all earthquakes. Triggering the SMA-MRF system, on the other hand, decreases the maximum displacement of the first storey of the structure for the simulated ground motions during the earthquakes in Christchurch, Parkfield, and Darfield to the values of 36, 24, and 13 mm, respectively. This equates to a decrease of 45.4%, 54.7%, and 71.7 per cent for the three earthquakes, respectively. Also, it has shown that the system can reduce the drift ratio, and by activating the control system below 0.8 Hz and deactivated above 1.7 Hz, the frequency response of the structure shifted into the safe zone for a wide range of loading frequencies.

A numerical study by Kecik [204] presented the application of Magneto-Rheological (MR) and SMA in a Pendulum Tuned Mass (PTM) absorber system with semi-active suspension. The main structure's vibration is suppressed by the pendulum motion, while the magnet oscillation generates a current in the harvester's coil. This system is surrounded by a magnetic field that is constant as illustrated in Fig. 25.

The SMA spring analysis indicated that increasing the temperature leads to a significant modification of the resonance curve shape. The application of SMA spring provided the possibility of unstable region control and an increase in energy recovery.

Huang and Chang [205] analysed the performance of a pre-stressed SMA applied to a timber floor system for semi-actively control of the tuned mass damper (Fig. 26). It was demonstrated that changing the temperature of an SMA can efficiently re-tune the structural natural frequency and reduce the vibration up to 26% at a wide range of frequencies.

Zuo et al. [206] considered using SMA strands to replace the spring and damper elements in the conventional TMD system to develop an SMA-based TMD to regulate the earthquake effects of turbine towers (Fig. 27). Their findings revealed that the mean maximum strokes of the SMA-based TMD at the top of the tower under the specified movements is 0.13 m, whereas the linear TMD is 0.77 m. Because of the limited area in the nacelle and tower, this benefit makes SMA-based TMDs more practicable for tower vibration reduction.

As illustrated in Fig. 28, Zhang et al. [207] proposed a unique form of hybrid self-centring brace that incorporates tension-only pseudoelastic Ni–Ti strands and embedded viscoelastic dampers. Maximum inter-storey drift measurements revealed that the SMA-viscoelastic hybrid bracing system had 35% lower values than the self-centring system. Furthermore, the SMA-viscoelastic hybrid bracing prototype demonstrated effective self-centring and energy-dissipation performance, despite the presence of residual strain owing to production imperfection.

7. Summary of practical examples of SMA-based structural vibration control devices

Section 6 contains a review of the most current investigations and their findings. Fig. 29 depicts a schematic classification of various applications depending on the technique and system employed. The SMA-based devices are divided into three categories: passive (based on the pseudoelasticity property of SMAs), active (based on the shape memory effect property of SMAs), and semi-active vibration control. The type of device and system is then presented in each category based on the accessible literature.

The majority of SMA applications in vibration control devices for civil engineering structures are based on the pseudoelasticity property, because of its simplicity of implementation in comparison to the shape memory effect (SME) feature. As a result, the variety of applications of the SME characteristic of SMAs as vibration control devices is limited. As a result, the SME characteristic might be employed more effectively

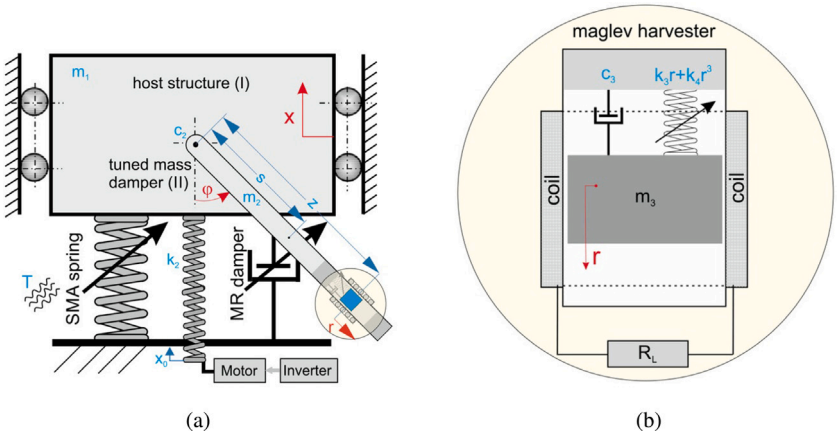

Fig. 25. (a) The vibration damper; (b) the maglev harvester model [204].

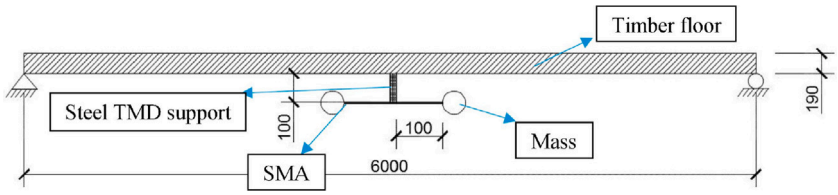

Fig. 26. Configuration of the SMA-based tuned mass damper [205].

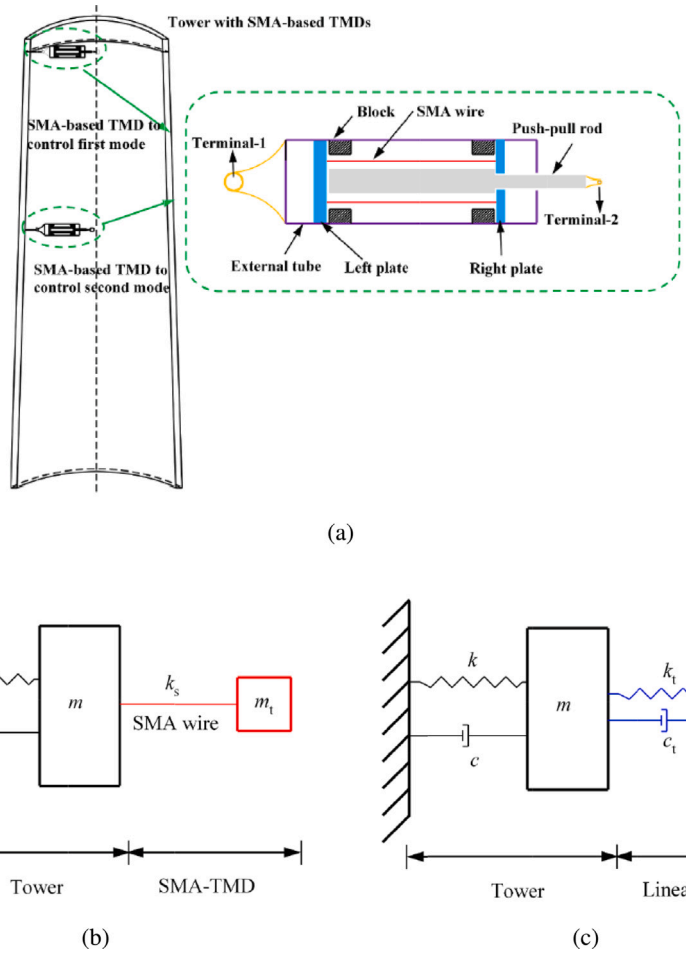

Fig. 27. Numerical simulations of the structure with SMA-based and linear TMDs and design development of SMA-based TMDs [206].

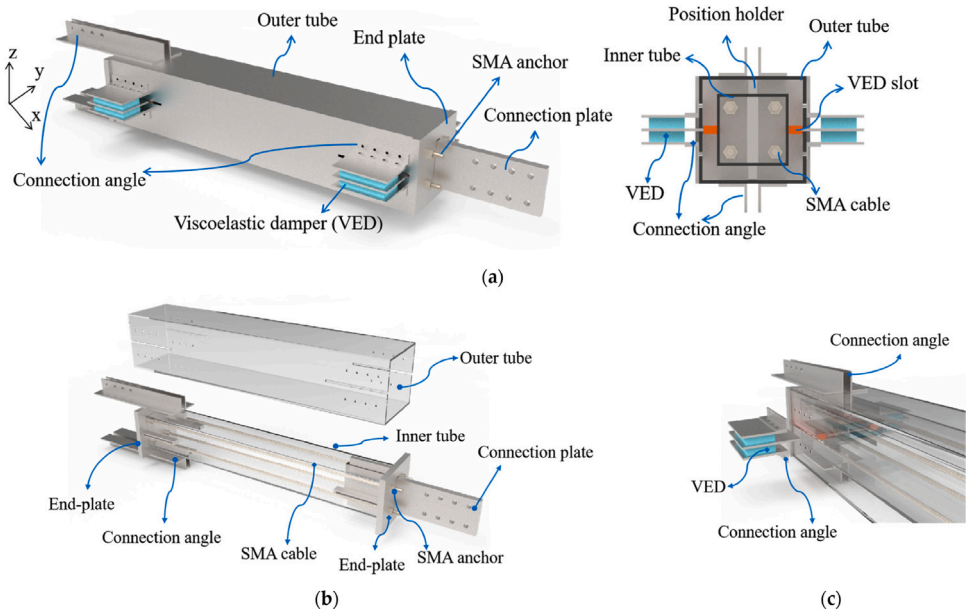

Fig. 28. Schematics of (a) SMA-viscoelastic hybrid braces, as well as its (b) self-centring system and (c) energy-dissipation system [207].

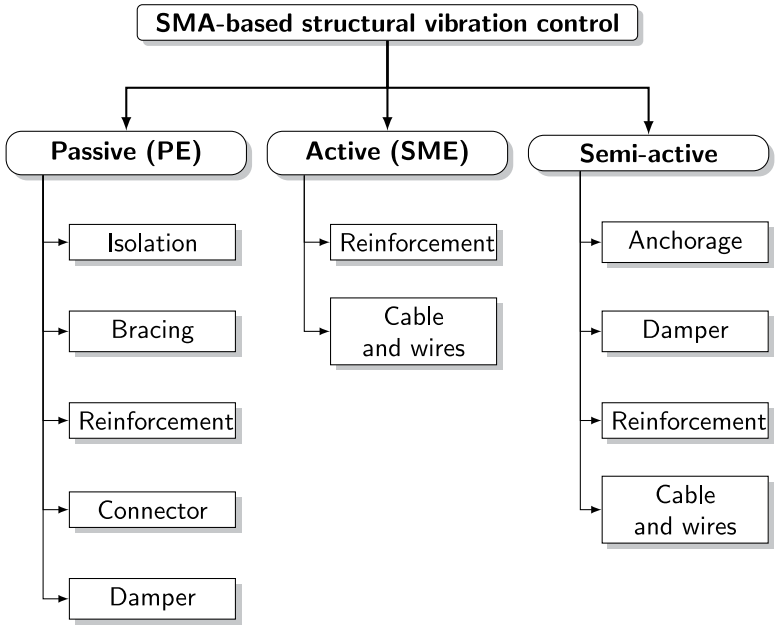

Fig. 29. Structural vibration control of SMA-based devices based on the used mechanism.

as an actuator in different types of vibration control systems and devices (e.g. TMD, MRF, viscoelastic damper, etc.).

Table 5 summarizes the different applications of SMA-based structural control systems reviewed in Section 6. The table divides the application of SMAs in vibration control of civil engineering structures based on the type, device and used mechanism. Additionally, in the last column, five features are assigned to each system, which are listed as following:

- (A) mechanism: based on shape-memory effect (A1); based on pseudoelasticity (A2)
- (B) cost: economical (B1); fair (B2); expensive (B3)
- (C) constructibility: easy (C1); moderate (C2); complicated (C3)
- (D) dissipation of energy: high (D1); moderate (D2); low (D3)
- (E) effectiveness: effective (E1); moderate (E2); limited (E3)

The first group of features (A1 and A2) is given to each system based on the exhibited SMA mechanism (SME or PE).

The second group of features (B1, B2, and B3) is related to the system's manufacturing and implementation expenditures, such as (i) the SMA material utilized (e.g., the cost of Ni–Ti is considerably higher than Cu- and Fe-based SMAs); (ii) the quantity of required material; and (iii) cost of installation (for example, the installation of a base isolator on a historical building is significantly costlier than retrofitting a concrete beam).

The next series of features (C1, C2, and C3) is based on the system's simplicity and constructability. For example, if the system may be used immediately without the requirement for additional mass, energy, or an activating system, it might be termed a simple system to build. A system that required a substantial amount of energy or mass, on the other hand, is deemed a difficult system to build.

Table 5
Summary of SMA-based structural control devices.

No	Device	Structure	Mechanism	Description	Features
1	SMA spring	Base isolation	Passive	SMA spring installed at the isolation level of a multi-storey steel frame [170]	A2, B3, C3, D2, E2
2	SMA-UDs	Base isolation	Passive	SMA-UDs integrated into a LRB with a lead core and with steel U shaped damper [171]	A2, B1, C2, D2, E2
3	SMA-LRB	Base isolation	Passive	Wrapped Fe-based SMA wires around the LRB in a symmetric double cross configuration [208]	A2, B1, C3, D1, E1
4	SMA-UFREI	Base isolation	Passive	Integrated SMA wires with unbonded fibre reinforced elastomeric isolator as isolation system for historical masonry church [176]	A2, B1, C2, D1, E1
5	SMA wire	Braced frames	Passive	Pseudoelastic SMA fuse used in steel-braced frame [177]	A2, B3, C1, D2, E2
6	SMA cable	Anchorage	Passive	SMA cables installed into two different anchorage systems [209]	A2, B3, C2, D2, E2
7	SMA fibre	Steel shear wall	Passive	SMA fibres added to different parts of the steel shear wall [178]	A2, B3, C3, D2, E3
8	SMA bolt	Steel Column	Passive	Post-tensioned SMA bolts installed directly on both sides of the column's base plate [179]	A2, B3, C1, D2, E2
9	SMA wire	Tie-rods	Passive	Pre-tensioned SMA wires joint with two circular steel plates [180]	A2, B2, C2, D1, E1
10	SMA cable	Braced frames	Passive	SMA cables combined with friction energy dissipation system [181]	A2, B2, C2, D2, E2
11	SMA bar	RC wall	Passive	In two-sided boundary zones, SMA bars are utilized as longitudinal reinforcement [182]	A2, B3, C1, D2, E2
12	SMA-EBF	Braced frames	Passive	LRB equipped with SMA bars, stiffeners and steel plates [183]	A2, B3, C3, D2, E3
13	SMA-X-KBFs	Braced frames	Passive	SMA bars utilized in the adjacent of steel beam–column connection [184]	A2, B3, C3, D2, E3
14	SMA-NSM	RC beam	Passive	RC beam retrofitted by Fe-SMA strips with NSM technique [185]	A2, B1, C1, D2, E1
15	SMA-NSM	RC column	Passive	RC bridge columns retrofitted with SMA-NSM technique [186]	A2, B1, C2, D2, E2
16	SMA damper	Wires	Passive	Wind-loaded tower line reinforced with SMA damper [188]	A2, B3, C3, D2, E3
17	SMA bolt	Steel connection	Passive	A performance-spectra-based approach for evaluating the earthquake resistance of Steel frames reinforces with SMA bolts [187]	A2, B3, C1, D2, E2
18	SMA wire	Beam	Active	Active vibration suppression of a flexible contriver beam by SMA actuators [195]	A1, B3, C2, D2, E2
19	SMA tendon	Beam	Active	Different series of obliquely connections of SMA tendons were used as actuators [196]	A1, B3, C3, D2, E3
20	SMA wire	Laminated beam	Active	SMA wires are utilized as actuators in a piezoceramic laminated flexible cantilever beam for active vibration control [197]	A1, B2, C2, -, E2
21	SMA wire	Sandwich beam	Active	SMA-embedded sandwich beam with functionally graded porous core and composite face layers [198]	–
22	SMA spiral	RC columns	Active	heat-activated prestressing SMA spirals combined with other confinements [210]	A1, B3, C1, D2, E2
23	SMA string	Ring	Semi-Active	Adjusting the boundary condition with a SMA actuator to regulate the stiffness of a frame spring [199]	A1, B2, C2, D1, E2
24	SMA-TMD	SMA springs	Semi-Active	Replacing the linear spring and viscous damper with a SMA-based spring [201]	A2, B3, C3, D2, E3
25	SMA-MRF	Marine platform	Semi-Active	Dissipate energy based on magnetorheological fluid (MRF) and pseudoelasticity properties of the system [202,211]	A2, B1, C2, D1, E1
26	PTM-SMA-MR	SMA springs	Semi-Active	Absorber device on the semi-active suspension [204]	A1, B2, C3, D2, E2
27	SMA-TMD	Timber-based	Semi-Active	Reducing the structural response through cooling and heating the SMA [205]	A2, B3, C1, D1, E2
28	SMA-viscoelastic	Anchorage	Semi-Active	incorporating tension-only pseudoelastic Ni–Ti strands and embedded viscoelastic dampers [207]	A2, B3, C2, D2, E2
29	SMA-TMD	Wires	Semi-Active	SMA spring instead of steel one in conventional TMD system [206]	A2, B1, C2, D1, E1

The fourth set of features (D1, D2, and D3) is depending on the system's energy dissipation capabilities. Because the damping of different systems can be hardly compared directly (different types of used construction material, structural system, loading circumstances, etc.), the damping ratio in the systems with SMA was compared to the conventional system.

The last set of features (E1, E2, and E3) is based on the system's effectiveness in vibration control of civil engineering structures. To assess the system's efficiency, a variety of criteria, in addition to those mentioned above, are evaluated: hysteresis and energy dissipation; peak drift; residual strain; and damping capability are considered.

It is noted that all of the investigations discussed in the preceding sections are significant and beneficial to this area of expertise. These five features are provided to compare the various vibration control systems. The future researchers may benefit from the presented comparison of different systems in determining the type of system and SMA material, recommended mechanism, and so on in order to efficiently use the SMA-based vibration control device.

As the above table demonstrated, much less research has been conducted on utilizing the two-way shape memory effect of SMAs due to their limitations mentioned in Section 2. The majority of the discussed SMA-based devices, on the other hand, were based on the pseudoelastic characteristic of SMAs. SMA passive structural control devices were primarily utilized in base isolators, bracing systems, couplings and connectors, reinforcement, and such applications. Active and semi-active structural control devices were developed primarily using the thermomechanical characteristics of SMA or in conjunction with other materials such as piezoelectric.

8. Concluding remarks

This study provided a current state-of-the-art review on the use of shape memory alloys in seismic response control systems. This novel material has numerous distinct characteristics that open up new avenues for the design and use of seismic devices for building and infrastructure systems. There has been tremendous progress in the numerical

modelling and practical use of SMAs in vibration response control of civil engineering structures. However, there are a few drawbacks that might be addressed.

In general, the findings of this study and the existing limits of the use of SMAs in structural vibration control may be stated as follows:

- Ni–Ti alloys have so far demonstrated to have the most appealing features for civil engineering applications, such as high re-centring ability, superior fatigue resistance, high tensile strength, high recoverable elongation, and several other advantages. However, because of the high production costs, as well as the delicate manufacturing process, its vast range of structural applications is limited. On the other hand, Fe-based SMAs have received a lot of attention since they exhibit quite similar behaviour to Ni–Ti but at a considerably lower production cost (8 to 12 times lower [99]), which is why they are referred to as low-cost SMAs.
- several Fe-based SMAs (e.g. Fe–Mn–Si–Cr) may be limited in their practical applications due to the transition temperature range they exhibited. They have an M_s near 0 °C and are consequently thermodynamically stable at room temperatures in civil engineering structures. Thus their tendency to form renewed martensite (when cooled or loaded), is a significant constraint for applications requiring constant stress or variable temperatures.
- SMA is highly vulnerable to integrational deviations (i.e. minor variations in the components of an accompanying grade alloy may completely change the mechanical features of the material). Additionally, SMA characteristics are temperature dependent due to the material's thermomechanical sensitiveness. Therefore it would be beneficial if the SMA could be integrated with common construction materials and other vibration control technologies for broader application in civil engineering constructions for long-lasting and robust structures.
- while SMA actuators have been effectively used to stabilize civil engineering structures, they have a distinct drawback: the behaviour of the SMA devices is mostly dependent on the characteristic of controllers used and how heat is provided and eliminated [212–215]. Sreekumar et al. [213] proposed numerous solutions to this challenge (e.g. using nonlinear controllers, using a fuzzy controller or neuro-fuzzy controller and controlling with resistance or force feedback). A further approach to resolving this issue is to employ pseudoelastic SMA, thanks to its shape-recovery capacity without the necessity of an additional heat supply [216]. Such characteristics involve (i) repetitive re-centring ability and loading peak that constrain force transmission to other elements of the structure at medium strain levels; (ii) supplemental damping due to flag-shaped hysteresis; (iii) stiffening at large strain levels due to stress-induced martensite configuration; (iv) and great low- and high-cycle fatigue properties. Because of this distinct behaviour, it is widely assumed that SMAs may be utilized to regulate the reaction of a building during seismic occurrences [214].
- despite tremendous progress in numerical simulations of SMAs over the last few decades, there are still a few issues that may be addressed: (i) many established constitutive models on SMA-based vibration control devices are restricted to a simple one-dimensional model; (ii) material constitutive models for SMAs possessing SE and SME properties should be more accurate with appropriate capacity to estimate their exact reactions, as well as the implementation of these constitutive models into design and computational analysis software for accurate assessment of SMA-based vibration control devices; (iii) there is a lack of accurate and current design standards for civil engineering structures designed and built with SMA-based devices, as well as inclusion into design regulations.

Declaration of competing interest

The authors declare that they have no known competing financial interests or personal relationships that could have appeared to influence the work reported in this paper.

Acknowledgment

The research was funded by the research projects of Poznan University of Technology (grant numbers: 0412/SBAD/0060, 0412/SBAD/0061 and 0411/SBAD/0006).

References

[1] R.C. Durgesh, Future trends in earthquake-resistant design of structures, Current Sci. (2000).
[2] F.Y. Cheng, H. Jiang, K. Lou, Smart Structures: Innovative Systems for Seismic Response Control, CRC Press, 2008.
[3] L.B. Vernon, H.M. Vernon, Process of manufacturing articles of thermoplastic synthetic resins, 1941.
[4] W.J. Buehler, R.C. Wiley, The properties of TiNi and associated phases, Tech. rep., UNITED STATES NAVAL ORDNANCE LABORATORY, 1961.
[5] A. Tabrizikahou, M. Hadzima-Nyarko, M. Kuczma, S. Lozančić, Application of shape memory alloys in retrofitting of masonry and Heritage structures based on their vulnerability revealed in the Bam 2003 earthquake, Materials 14 (16) (2021) http://dx.doi.org/10.3390/ma14164480.
[6] H. Davoodi, F.A. Just, A. Saffar, M. Noori, Building system using shape memory alloy members, (Patent No.: US 6,170,202) United States Patent, 2001.
[7] S. Saadat, M. Noori, H. Davoodi, Z. Hou, Y. Suzuki, A. Masuda, Using NiTi SMA tendons for vibration control of coastal structures, Smart Mater. Struct. 10 (4) (2001) 695–704, http://dx.doi.org/10.1088/0964-1726/10/4/313.
[8] A. Sato, K. Soma, E. Chishima, T. Mori, Shape memory effect and mechanical behaviour of an Fe-30Mn-1Si alloy single crystal, Le J. Phys. Colloques 43 (1982) http://dx.doi.org/10.1051/jphyscol:19824130.
[9] R. Dasgupta, A look into Cu-based shape memory alloys: Present scenario and future prospects, J. Mater. Res. 29 (16) (2014) 1681–1698, http://dx.doi.org/10.1557/jmr.2014.189.
[10] A. Cladera, L.A. Montoya-Coronado, J.G. Ruiz-Pinilla, C. Ribas, Shear strengthening of slender reinforced concrete T-shaped beams using iron-based shape memory alloy strips, Eng. Struct. 221 (2020) 111018, http://dx.doi.org/10.1016/j.engstruct.2020.111018.
[11] S. Saadat, J. Salichs, M. Noori, Z. Hou, H. Davoodi, I. Bar-on, Y. Suzuki, A. Masuda, An overview of vibration and seismic applications of NiTi shape memory alloy, Smart Mater. Struct. 11 (2) (2002) 218–229, http://dx.doi.org/10.1088/0964-1726/11/2/305.
[12] K. Tanaka, F. Nishimura, M. Matsui, H. Tobushi, P.-H. Lin, Phenomenological analysis of plateaus on stress-strain hysteresis in TiNi shape memory alloy wires, Mech. Mater. 24 (1) (1996) 19–30, http://dx.doi.org/10.1016/0167-6636(96)00030-0.
[13] K. Tanaka, F. Nishimura, T. Hayashi, H. Tobushi, C. Lexcellent, Phenomenological analysis on subloops and cyclic behavior in shape memory alloys under mechanical and/or thermal loads, Mech. Mater. 19 (4) (1995) http://dx.doi.org/10.1016/0167-6636(94)00038-I.
[14] M. Niezgódka, J. Sprekels, Existence of solutions for a mathematical model of structural phase transitions in shape memory alloys, Math. Methods Appl. Sci. 10 (3) (1988) 197–223, http://dx.doi.org/10.1002/mma.1670100302.
[15] I. Muller, H. Xu, On the pseudo-elastic hysteresis, Acta Metall. Mater. 39 (3) (1991) 263–271, http://dx.doi.org/10.1016/0956-7151(91)90305-K.
[16] C. Lexcellent, H. Tobushi, Internal loops in pseudoelastic behaviour of Ti-Ni shape memory alloys: Experiment and modelling, Meccanica 30 (5) (1995) 459–466, http://dx.doi.org/10.1007/BF01557078.
[17] R. Desroches, B. Smith, Shape memory alloys in seismic resistant design and retrofit: A critical review of their potential and limitations, J. Earthq. Eng. 8 (3) (2004) 415–429, http://dx.doi.org/10.1080/13632460409350495.
[18] J.C. Wilson, M.J. Wesolowsky, Shape memory alloys for seismic response modification: A state-of-the-art review, Earthq. Spectra 21 (2) (2005) 569–601, http://dx.doi.org/10.1193/1.1897384.
[19] H. Qian, H.N. Li, G. Song, H. Chen, W.J. Ren, S. Zhang, Seismic vibration control of civil structures using shape memory alloys: A review, in: Earth and Space, pp. 3377–3395, http://dx.doi.org/10.1061/41096(366)322.
[20] E.J. Graesser, F.A. Cozzarelli, Shape memory alloys as new materials for Aseismic isolation, J. Eng. Mech. 117 (11) (1991) 2590–2608, http://dx.doi.org/10.1061/(ASCE)0733-9399(1991)117:11(2590).
[21] E. Graesser, F. Cozzarelli, A proposed three-dimensional constitutive model for shape memory alloys, J. Intell. Mater. Syst. Struct. 5 (1) (1994) 78–89, http://dx.doi.org/10.1177/1045389X9400500109.

[22] K. Wilde, P. Gardoni, Y. Fujino, Seismic response of base-isolated structures with shape memory alloy damping devices, in: N. Stubbs (Ed.), Smart Structures and Materials 1997: Smart Systems for Bridges, Structures, and Highways, Vol. 3043, SPIE, 1997, pp. 122–133, http://dx.doi.org/10.1117/12.274648.

[23] O.E. Ozbulut, S. Hurlebaus, R. Desroches, Seismic response control using shape memory alloys: A review, J. Intell. Mater. Syst. Struct. 22 (14) (2011) 1531–1549, http://dx.doi.org/10.1177/1045389X11411220.

[24] S. Zareie, A.S. Issa, R.J. Seethaler, A. Zabihollah, Recent advances in the applications of shape memory alloys in civil infrastructures: A review, Structures 27 (2020) 1535–1550, http://dx.doi.org/10.1016/j.istruc.2020.05.058.

[25] A. Muntasir Billah, J. Rahman, Q. Zhang, Shape memory alloys (SMAs) for resilient bridges: A state-of-the-art review, Structures 37 (2022) 514–527, http://dx.doi.org/10.1016/j.istruc.2022.01.034.

[26] A. Tabrizikahou, M. Kuczma, P. Nowotarski, M. Kwiatek, A. Javanmardi, Sustainability of civil structures through the application of smart materials: A review, Materials 14 (17) (2021) http://dx.doi.org/10.3390/ma14174824.

[27] L. Duval, M. Noori, Z. Hou, H. Davoodi, S. Seelecke, Random vibration studies of an SDOF system with shape memory restoring force, Physica B 275 (1) (2000) 138–141, http://dx.doi.org/10.1016/S0921-4526(99)00721-8.

[28] B. Raniecki, C. Lexcellent, K. Tanaka, Thermodynamic models of pseudoelastic behaviour of shape memory alloys, Arch. Mech. 44 (1992) 261–284.

[29] F. Auricchio, R.L. Taylor, J. Lubliner, Shape-memory alloys: macromodelling and numerical simulations of the superelastic behavior, Comput. Methods Appl. Mech. Engrg. 146 (3) (1997) 281–312, http://dx.doi.org/10.1016/S0045-7825(96)01232-7.

[30] M. Kuczma, A. Mielke, Influence of hardening and inhomogeneity on internal loops in pseudoelasticity, ZAMM Z. Angew. Math. Mech. 80 (2000) 291–306.

[31] M. Kuczma, A. Mielke, E. Stein, Modelling of hysteresis in two phase systems, Arch. Mech. 51 (1999) 693–715.

[32] W. Huang, W. Toh, Training two-way shape memory alloy by reheat treatment, J. Mater. Sci. Lett. 19 (17) (2000) 1549–1550, http://dx.doi.org/10.1023/A:1006721022185.

[33] J. Ma, I. Karaman, R.D. Noebe, High temperature shape memory alloys, Int. Mater. Rev. 55 (5) (2010) 257–315, http://dx.doi.org/10.1179/095066010X12646898728363.

[34] F. Nematzadeh, S. Sadrnezhaad, Effects of material properties on mechanical performance of nitinol stent designed for femoral artery: Finite element analysis, Sci. Iran. 19 (6) (2012) 1564–1571, http://dx.doi.org/10.1016/j.scient.2012.10.024.

[35] Y.H. Wen, H.B. Peng, D. Raabe, I. Gutierrez-Urrutia, J. Chen, Y.Y. Du, Large recovery strain in fe-mn-si-based shape memory steels obtained by engineering annealing twin boundaries, Nature Commun. 5 (1) (2014) 4964, http://dx.doi.org/10.1038/ncomms5964.

[36] A. Agrawal, S.K. Vajpai, Preparation of Cu–Al–Ni shape memory alloy strips by spray deposition-hot rolling route, Mater. Sci. Technol. 36 (12) (2020) 1337–1348, http://dx.doi.org/10.1080/02670836.2020.1781354.

[37] M.F. McGuire, Stainless Steels for Design Engineers, ASM International, 2008.

[38] K. Otsuka, C.M. Wayman, Shape Memory Materials, Cambridge University Press, 1999.

[39] A. Cladera, B. Weber, C. Leinenbach, C. Czaderski, M. Shahverdi, M. Motavalli, Iron-based shape memory alloys for civil engineering structures: An overview, Constr. Build. Mater. 63 (2014) 281–293, http://dx.doi.org/10.1016/j.conbuildmat.2014.04.032.

[40] M.K. Abbass, M.M. Radhi, R.S.A. Adnan, The effect of germanium addition on mechanical properties and microstructure of Cu-Al-Ni shape memory alloy, Mater. Today: Proc. 4 (2, Part A) (2017) 224–233, http://dx.doi.org/10.1016/j.matpr.2017.01.016, 5th International Conference of Materials Processing and Characterization (ICMPC 2016).

[41] I. Tolosa, F. Garciandía, F. Zubiri, F. Zapirain, A. Esnaola, Study of mechanical properties of AISI 316 stainless steel processed by "selective laser melting", following different manufacturing strategies, Int. J. Adv. Manuf. Technol. 51 (5–8) (2010) 639–647, http://dx.doi.org/10.1007/s00170-010-2631-5.

[42] N. Kurgan, R. Varol, Mechanical properties of P/M 316L stainless steel materials, Powder Technol. 201 (3) (2010) 242–247, http://dx.doi.org/10.1016/j.powtec.2010.03.041.

[43] P. Šittner, L. Heller, J. Pilch, C. Curfs, T. Alonso, D. Favier, Young'S modulus of austenite and martensite phases in superelastic NiTi wires, J. Mater. Eng. Perform. 23 (7) (2014) 2303–2314, http://dx.doi.org/10.1007/s11665-014-0976-x.

[44] D. Abolhasani, S.W. Han, C.J. VanTyne, N. Kang, Y.H. Moon, Enhancing the shape memory effect of Cu–Al–Ni alloys via partial reinforcement by alumina through selective laser melting, J. Mater. Res. Technol. 15 (2021) 4032–4047, http://dx.doi.org/10.1016/j.jmrt.2021.10.040.

[45] A. Lebedev, V. Kosarchuk, Influence of phase transformations on the mechanical properties of austenitic stainless steels, Int. J. Plast. 16 (7–8) (2000) 749–767, http://dx.doi.org/10.1016/S0749-6419(99)00085-6.

[46] Z. Wang, J. Everaerts, E. Salvati, A.M. Korsunsky, Evolution of thermal and mechanical properties of nitinol wire as a function of ageing treatment conditions, J. Alloys Compd. 819 (2020) 153024, http://dx.doi.org/10.1016/j.jallcom.2019.153024.

[47] C. Leinenbach, H. Kramer, C. Bernhard, D. Eifler, Thermo-mechanical properties of an Fe-Mn-Si-Cr-Ni-VC shape memory alloy with low transformation temperature, Adv. Energy Mater. 14 (1–2) (2012) 62–67, http://dx.doi.org/10.1002/adem.201100129.

[48] I. Ruiz-Larrea, A. López-Echarri, E. Bocanegra, M. Nó, J. San Juan, The specific heat of Cu–Al–Ni shape memory alloys, Mater. Sci. Eng. A 438–440 (2006) 779–781, http://dx.doi.org/10.1016/j.msea.2006.02.099.

[49] L. Leibowitz, R.A. Blomquist, Thermal conductivity and thermal expansion of stainless steels D9 and HT9, Int. J. Thermophys. 9 (5) (1988) 873–883, http://dx.doi.org/10.1007/BF00503252.

[50] J.L. McNichols, J.S. Cory, Thermodynamics of Nitinol, J. Appl. Phys. 61 (3) (1987) 972–984, http://dx.doi.org/10.1063/1.338151.

[51] V. Recarte, J. Pérez-Landazábal, P. Rodrıguez, E. Bocanegra, M. Nó, J. San Juan, Thermodynamics of thermally induced martensitic transformations in Cu–Al–Ni shape memory alloys, Acta Mater. 52 (13) (2004) 3941–3948, http://dx.doi.org/10.1016/j.actamat.2004.05.009, URL https://linkinghub.elsevier.com/retrieve/pii/S135964540400271X.

[52] J. Gallardo Fuentes, P. Gümpel, J. Strittmatter, Phase change behavior of Nitinol shape memory alloys, Adv. Energy Mater. 4 (7) (2002) 437–452, http://dx.doi.org/10.1002/1527-2648(20020717)4:7<437::AID-ADEM437>3.0.CO;2-8.

[53] T. Mohri, Y. Chen, M. Kohyama, S. Ogata, A. Saengdeejing, S.K. Bhattacharya, M. Wakeda, S. Shinzato, H. Kimizuka, Mechanical properties of Fe-rich Si alloy from Hamiltonian, Npj Comput. Mater. 3 (1) (2017) 10, http://dx.doi.org/10.1038/s41524-017-0012-4.

[54] B. Duran, K.C. Atlı, O. Avşar, Superelastic cyclic properties of Cu-Al-Mn and Ni-Ti shape memory alloys for seismic mitigation, 2020, http://dx.doi.org/10.11159/icsect20.117, URL https://avestia.com/CSEE2020_Proceedings/files/paper/ICSECT/ICSECT_117.pdf.

[55] H. Cao, M.H. Wu, F. Zhou, R.M. McMeeking, R.O. Ritchie, The influence of mean strain on the high-cycle fatigue of Nitinol with application to medical devices, J. Mech. Phys. Solids 143 (2020) 104057, http://dx.doi.org/10.1016/j.jmps.2020.104057.

[56] M. Mahtabi, N. Shamsaei, B. Rutherford, Mean strain effects on the fatigue behavior of superelastic nitinol alloys: An experimental investigation, Procedia Eng. 133 (2015) 646–654, http://dx.doi.org/10.1016/j.proeng.2015.12.645.

[57] X. Zhang, D. Wang, Y. Zhou, X. Chong, X. Li, H. Zhang, H. Nagaumi, Exploring crystal structures, stability and mechanical properties of Fe, Mn-containing intermetallics in Al-Si alloy by experiments and first-principles calculations, J. Alloys Compd. 876 (2021) 160022, http://dx.doi.org/10.1016/j.jallcom.2021.160022.

[58] U. Sarı, T. Kırındı, Effects of deformation on microstructure and mechanical properties of a Cu–Al–Ni shape memory alloy, Mater. Charact. 59 (7) (2008) 920–929, http://dx.doi.org/10.1016/j.matchar.2007.07.017, URL https://linkinghub.elsevier.com/retrieve/pii/S1044580307002677.

[59] S. Tsopanos, R.A.W. Mines, S. McKown, Y. Shen, W.J. Cantwell, W. Brooks, C.J. Sutcliffe, The influence of processing parameters on the mechanical properties of selectively laser melted stainless steel microlattice structures, J. Manuf. Sci. Eng. 132 (4) (2010) http://dx.doi.org/10.1115/1.4001743.

[60] R.-b. Song, J.-y. Xiang, D.-p. Hou, Characteristics of mechanical properties and microstructure for 316L austenitic stainless steel, J. Iron Steel Res. Int. 18 (11) (2011) 53–59, http://dx.doi.org/10.1016/S1006-706X(11)60117-9.

[61] A. Bhardwaj, A.K. Gupta, S.K. Padisala, K. Poluri, Characterization of mechanical and microstructural properties of constrained groove pressed nitinol shape memory alloy for biomedical applications, Mater. Sci. Eng. C 102 (2019) 730–742, http://dx.doi.org/10.1016/j.msec.2019.04.070.

[62] A. Druker, A. Perotti, I. Esquivel, J. Malarría, Design of devices and manufacturing of Fe-Mn-Si shape memory alloy couplings, Proc. Mater. Sci. 8 (2015) 878–885, http://dx.doi.org/10.1016/j.mspro.2015.04.148.

[63] I. López-Ferreño, J. Gómez-Cortés, T. Breczewski, I. Ruiz-Larrea, M. Nó, J. San Juan, High-temperature shape memory alloys based on the Cu-Al-Ni system: design and thermomechanical characterization, J. Mater. Res. Technol. 9 (5) (2020) 9972–9984, http://dx.doi.org/10.1016/j.jmrt.2020.07.002, URL https://linkinghub.elsevier.com/retrieve/pii/S2238785420315003.

[64] Q. Zhang, B. Cui, B. Sun, X. Zhang, Z. Dong, Q. Liu, T. Cui, Effect of sm doping on the microstructure, mechanical properties and shape memory effect of Cu-13.0Al-4.0Ni alloy, Materials 14 (14) (2021) 4007, http://dx.doi.org/10.3390/ma14144007.

[65] P. Marshall, Austenitic Stainless Steels: Microstructure and Mechanical Properties, Springer Science & Business Media, 1984.

[66] M. Azaouzi, N. Lebaal, A. Makradi, S. Belouettar, Optimization based simulation of self-expanding Nitinol stent, Mater. Des. 50 (2013) 917–928, http://dx.doi.org/10.1016/j.matdes.2013.03.012.

[67] N. Stanford, D. Dunne, Thermo-mechanical processing and the shape memory effect in an Fe–Mn–Si-based shape memory alloy, Mater. Sci. Eng. A 422 (1) (2006) 352–359, http://dx.doi.org/10.1016/j.msea.2006.02.009.

[68] I. Milošev, B. Kapun, The corrosion resistance of nitinol alloy in simulated physiological solutions, Mater. Sci. Eng. C 32 (5) (2012) 1087–1096, http://dx.doi.org/10.1016/j.msec.2011.11.007.

[69] L. Baroni, R. Silva, G. Vacchi, V. Sordi, C. Rovere, Influence of ce on the corrosion properties of fe-mn-si-based shape memory stainless steel, Mater.Today Commun. 25 (2020) 101649, http://dx.doi.org/10.1016/j.mtcomm.2020.101649.

[70] H. Otsuka, H. Yamada, T. Maruyama, H. Tanahashi, S. Matsuda, M. Murakami, Effects of alloying additions on fe-mn-si shape memory alloys, ISIJ Int. 30 (8) (1990) 674–679, http://dx.doi.org/10.2355/isijinternational.30.674.

[71] P. Parameswaran, A. Rameshbabu, G. Navaneetha Krishnan, R. Yogeshwaran, R. Ramkumar, Study of the corrosion properties in a hot forged Cu-Al-Ni alloy with added Cr, J. Mech. Behav. Mater. 27 (3–4) (2018) http://dx.doi.org/10.1515/jmbm-2018-0016.

[72] A.S.M. Najib, S.N. Saud, E. Hamzah, Corrosion behavior of Cu–Al–Ni–xCo shape memory alloys coupled with low-carbon steel for civil engineering applications, J. Bio- Tribo-Corrosion 5 (2) (2019) 47, http://dx.doi.org/10.1007/s40735-019-0242-8.

[73] A. Sedriks, Corrosion of stainless steels, in: Encyclopedia of Materials: Science and Technology, Elsevier, 2001, pp. 1707–1708, http://dx.doi.org/10.1016/B0-08-043152-6/00304-1.

[74] S.W. Robertson, A.R. Pelton, R.O. Ritchie, Mechanical fatigue and fracture of Nitinol, Int. Mater. Rev. 57 (1) (2012) 1–37, http://dx.doi.org/10.1179/1743280411Y.0000000009.

[75] R. Dasgupta, A.K. Jain, P. Kumar, S. Hussain, A. Pandey, Role of alloying additions on the properties of Cu–Al–Mn shape memory alloys, J. Alloys Compd. 620 (2015) 60–66, http://dx.doi.org/10.1016/j.jallcom.2014.09.047.

[76] G. Song, N. Ma, H.N. Li, Applications of shape memory alloys in civil structures, Eng. Struct. (2006) http://dx.doi.org/10.1016/j.engstruct.2005.12.010.

[77] A. Baruj, T. Kikuchi, S. Kajiwara, N. Shinya, Improved shape memory properties and internal structures in Fe-Mn-Si-based alloys containing Nb and C, J. Phys. IV (Proceedings) 112 (2003) 373–376, http://dx.doi.org/10.1051/jp4:2003904.

[78] A.O. Moghaddam, M. Ketabchi, R. Bahrami, Kinetic grain growth, shape memory and corrosion behavior of two Cu-based shape memory alloys after thermomechanical treatment, Trans. Nonferr. Met. Soc. China 23 (10) (2013) 2896–2904, http://dx.doi.org/10.1016/S1003-6326(13)62812-5.

[79] D.E. Hodgson, M.H. Wu, R.J. Biermann, Shape memory alloys, in: Properties and Selection: Nonferrous Alloys and Special-Purpose Materials, ASM International, 1990, pp. 897–902, http://dx.doi.org/10.31399/asm.hb.v02.a0001100.

[80] T. Omori, S. Abe, Y. Tanaka, D. Lee, K. Ishida, R. Kainuma, Thermoelastic martensitic transformation and superelasticity in Fe–Ni–Co–Al–Nb–B polycrystalline alloy, Scr. Mater. 69 (11–12) (2013) 812–815, http://dx.doi.org/10.1016/j.scriptamat.2013.09.006.

[81] Y. Tanaka, Y. Himuro, R. Kainuma, Y. Sutou, T. Omori, K. Ishida, Ferrous polycrystalline shape-memory alloy showing huge superelasticity, Science 327 (5972) (2010) 1488–1490, http://dx.doi.org/10.1126/science.1183169.

[82] Y. Sutou, T. Omori, R. Kainuma, K. Ishida, N. Ono, Enhancement of superelasticity in Cu-Al-Mn-Ni shape-memory alloys by texture control, Metall. Mater. Trans. A 33 (9) (2002) 2817–2824, http://dx.doi.org/10.1007/s11661-002-0267-2.

[83] Z.G. Wei, R. Sandstrom, S. Miyazaki, Shape memory materials and hybrid composites for smart systems: Part II shape-memory hybrid composites, J. Mater. Sci. 33 (15) (1998) 3763–3783, http://dx.doi.org/10.1023/A:1004674630156.

[84] H. Peng, J. Chen, S. Wang, Y. Wen, Effect of carbon addition on recovery behavior of trained Fe-Mn-Si based shape memory alloys, Adv. Energy Mater. 17 (2) (2015) 205–210, http://dx.doi.org/10.1002/adem.201400193.

[85] M. Guerioune, Y. Amiour, W. Bounour, O. Guellati, A. Benaldjia, A. Amara, N.E. Chakri, M. Ali-Rachedi, D. Vrel, SHS Of shape memory CuZnAl alloys, Int. J. Self-Propagating High-Temp. Synthesis 17 (1) (2008) 41–48, http://dx.doi.org/10.3103/S1061386208010044.

[86] A. Jalaeefar, B. Asgarian, Experimental investigation of mechanical properties of Nitinol, structural steel, and their hybrid component, J. Mater. Civ. Eng. 25 (10) (2013) 1498–1505, http://dx.doi.org/10.1061/(ASCE)MT.1943-5533.0000701.

[87] M.R. Rezvani, A. Shokuhfar, Synthesis and characterization of nano structured Cu–Al–Mn shape memory alloy by mechanical alloying, Mater. Sci. Eng. A 532 (2012) 282–286, http://dx.doi.org/10.1016/j.msea.2011.10.093, URL https://linkinghub.elsevier.com/retrieve/pii/S0921509311011956.

[88] N. Surendran, A. Varma, Buckling restrained braces (BRB)–a review, Int. Res. J. Eng. Technol. (IRJET) 4 (3) (2017) 2320–2324.

[89] Q. Chen, B. Andrawes, Cyclic stress-strain behavior of concrete confined with NiTiNb-shape memory alloy spirals, J. Struct. Eng. 143 (5) (2017) 04017008, http://dx.doi.org/10.1061/(ASCE)ST.1943-541X.0001728.

[90] D. Shanmuga Priya, A. Cinitha, P. Umesha, R.I. Nagesh, Enhancing the seismic response of buildings with energy dissipation methods–an overview, J. Civ. Eng. Res. (2014).

[91] A. Tabrizikahou, M. Kuczma, M. Łasecka Plura, E. Noroozinejad Farsangi, Cyclic behavior of masonry shear walls retrofitted with engineered cementitious composite and pseudoelastic shape memory alloy, Sensors 22 (2) (2022) http://dx.doi.org/10.3390/s22020511.

[92] M.R. Rezvani, A. Shokuhfar, Synthesis and characterization of nano structured Cu–Al–Mn shape memory alloy by mechanical alloying, Mater. Sci. Eng. A 532 (2012) 282–286, http://dx.doi.org/10.1016/j.msea.2011.10.093.

[93] Y. Liu, J. Van Humbeeck, R. Stalmans, L. Delaey, Some aspects of the properties of NiTi shape memory alloy, J. Alloys Compd. 247 (1–2) (1997) 115–121, http://dx.doi.org/10.1016/S0925-8388(96)02572-8.

[94] D. Wolons, F. Gandhi, B. Malovrh, Experimental investigation of the pseudoelastic hysteresis damping characteristics of shape memory alloy wires, J. Intell. Mater. Syst. Struct. 9 (2) (1998) 116–126, http://dx.doi.org/10.1177/1045389X9800900205.

[95] A.S. Whittaker, Structural Control of Buildings Response using Shape-Memory Alloys, US Army Construction Engineering Research Laboratory, 1995.

[96] J. Inaudi, J. Kelly, Experiments on tuned mass dampers using viscoelastic, frictional and shape-memory alloy materials, in: First World Conference on Structural Control, Los Angeles, USA, 1994, pp. 127–136.

[97] M. Dolce, D. Cardone, Mechanical behaviour of shape memory alloys for seismic applications 2. austenite NiTi wires subjected to tension, Int. J. Mech. Sci. 43 (11) (2001) 2657–2677, http://dx.doi.org/10.1016/S0020-7403(01)00050-9.

[98] J.V. Humbeeck, J. Stoiber, L. Delaey, R. Gotthardt, The high damping capacity of shape memory alloys, Int. J. Mater. Res. 86 (3) (1995) 176–183, http://dx.doi.org/10.1515/ijmr-1995-860306.

[99] L. Janke, C. Czaderski, M. Motavalli, J. Ruth, Applications of shape memory alloys in civil engineering structures—Overview, limits and new ideas, Mater. Struct. 38 (5) (2005) 578–592, http://dx.doi.org/10.1007/BF02479550.

[100] W. Wang, C. Fang, A. Zhang, X. Liu, Manufacturing and performance of a novel self-centring damper with shape memory alloy ring springs for seismic resilience, Struct. Control Health Monit. 26 (5) (2019) http://dx.doi.org/10.1002/stc.2337.

[101] K.K. Alaneme, T.J. Ubah, E.O. Aikulola, On the material characteristics of Ni modified Cu32Zn10Sn shape memory alloys: Mechanical and damping behaviour in consideration, Mater. Today: Proc. (2022) http://dx.doi.org/10.1016/j.matpr.2022.02.090.

[102] I. Ivanić, S. Kožuh, T.H. Grgurić, L. Vrsalović, M. Gojić, The effect of heat treatment on damping capacity and mechanical properties of CuAlNi shape memory alloy, Materials 15 (5) (2022) 1825, http://dx.doi.org/10.3390/ma15051825.

[103] G. Eggeler, E. Hornbogen, A. Yawny, A. Heckmann, M. Wagner, Structural and functional fatigue of NiTi shape memory alloys, Mater. Sci. Eng. A 378 (1) (2004) 24–33, http://dx.doi.org/10.1016/j.msea.2003.10.327, European Symposium on Martensitic Transformation and Shape-Memory.

[104] E. Hornbogen, Review thermo-mechanical fatigue of shape memory alloys, J. Mater. Sci. 39 (2) (2004) 385–399, http://dx.doi.org/10.1023/B:JMSC.0000011492.88523.d3.

[105] Z. Xie, Y. Liu, J. Van Humbeeck, Microstructure of NiTi shape memory alloy due to tension–compression cyclic deformation, Acta Mater. 46 (6) (1998) 1989–2000, http://dx.doi.org/10.1016/S1359-6454(97)00379-0.

[106] Y. Liu, Z. Xie, J. Van Humbeeck, Cyclic deformation of NiTi shape memory alloys, Mater. Sci. Eng. A 273–275 (1999) 673–678, http://dx.doi.org/10.1016/S0921-5093(99)00347-0.

[107] S. Miyazaki, Thermal and stress cycling effects and fatigue properties of Ni-Ti alloys, in: T.W. Duerig, K.N. Melton, D. Stöckel, C.M. Wayman (Eds.), Engineering Aspects of Shape Memory Alloys, Butterworth-Heinemann, 1990, pp. 394–413, http://dx.doi.org/10.1016/B978-0-7506-1009-4.50037-8.

[108] H. Tobushi, H. Iwanaga, K. Tanaka, T. Hori, T. Sawada, Stress-strain-temperature relationships of tini shape memory alloy suitable for thermomechanical cycling, JSME int. j. Ser. 1, Solid mech. strength mater. 35 (3) (1992) 271–277, http://dx.doi.org/10.1299/jsmea1988.35.3_271.

[109] C. Picornell, E. Cesari, M. Sade, Characteristics of the martensitic transformation and the induced two-way shape memory effect after training by compressive pseudoelastic cycling in Cu-Zn-Al single crystals, Metall. Mater. Trans. A 25 (4) (1994) 687–695, http://dx.doi.org/10.1007/BF02665445.

[110] H. Tobushi, S. Yamada, T. Hachisuka, A. Ikai, K. Tanaka, Thermomechanical properties due to martensitic and R-phase transformations of TiNi shape memory alloy subjected to cyclic loadings, Smart Mater. Struct. 5 (6) (1996) 788–795, http://dx.doi.org/10.1088/0964-1726/5/6/008.

[111] J. Van Humbeeck, Non-medical applications of shape memory alloys, Mater. Sci. Eng. A 273–275 (1999) 134–148, http://dx.doi.org/10.1016/S0921-5093(99)00293-2.

[112] R. DesRoches, J. McCormick, M. Delemont, Cyclic properties of superelastic shape memory alloy wires and bars, J. Struct. Eng. 130 (1) (2004) 38–46, http://dx.doi.org/10.1061/(ASCE)0733-9445(2004)130:1(38).

[113] C. Friend, N. Morgan, Fatigue/cyclic stability of shape-memory alloys, in: SMST-99: 1st European Conf. on Shape Memory and Superelasticity, Atwerp Zoo, Belgium, 1999, pp. 115–128.

[114] H. Scherngell, A. Kneissl, Influence of the microstructure on the stability of the intrinsic two-way shape memory effect, Mater. Sci. Eng. A 273–275 (1999) 400–403, http://dx.doi.org/10.1016/S0921-5093(99)00306-8.

[115] B. Wang, S. Zhu, Cyclic tension–compression behavior of superelastic shape memory alloy bars with buckling-restrained devices, Constr. Build. Mater. 186 (2018) 103–113, http://dx.doi.org/10.1016/j.conbuildmat.2018.07.047.

[116] F. Shi, O.E. Ozbulut, Z. Li, Z. Wu, F. Ren, Y. Zhou, Effects of ambient temperature on cyclic response and functional fatigue of shape memory alloy cables, J. Build. Eng. (2022) 104340, http://dx.doi.org/10.1016/j.jobe.2022.104340.

[117] K. Wu, F. Yang, Z. Pu, J. Shi, The effect of strain rate on detwinning and superelastic behavior of Ni ti shape memory alloys, J. Intell. Mater. Syst. Struct. 7 (2) (1996) 138–144, http://dx.doi.org/10.1177/1045389X9600700203.

[118] V. Kolomytsev, A. Kozlov, A. Seerneels, W. Moorleghm, D. Aslanidis, Effect of strain rate and sample size on features of non-linear deformation behaviour in TiNi-based ribbons and wires, in: XXYIII Symposium of UIA, May, 1998, pp. 13–15.

[119] H. Tobushi, Y. Shimeno, T. Hachisuka, K. Tanaka, Influence of strain rate on superelastic properties of TiNi shape memory alloy, Mech. Mater. 30 (2) (1998) 141–150, http://dx.doi.org/10.1016/S0167-6636(98)00041-6.

[120] H. Soul, A. Isalgue, A. Yawny, V. Torra, F.C. Lovey, Pseudoelastic fatigue of NiTi wires: frequency and size effects on damping capacity, Smart Mater. Struct. 19 (8) (2010) 085006, http://dx.doi.org/10.1088/0964-1726/19/8/085006.

[121] B. Strnadel, S. Ohashi, H. Ohtsuka, T. Ishihara, S. Miyazaki, Cyclic stress-strain characteristics of Ti-Ni and Ti-Ni-Cu shape memory alloys, Mater. Sci. Eng. A 202 (1) (1995) 148–156, http://dx.doi.org/10.1016/0921-5093(95)09801-1.

[122] S. Motahari, M. Ghassemieh, S. Abolmaali, Implementation of shape memory alloy dampers for passive control of structures subjected to seismic excitations, J. Construct. Steel Res. 63 (12) (2007) 1570–1579, http://dx.doi.org/10.1016/j.jcsr.2007.02.001.

[123] K. Wilde, Y. Zheng, P. Gardoni, Y. Fujino, Experimental and analytical study on a shape memory alloy damper, in: S.-C. Liu (Ed.), Smart Structures and Materials 1998: Smart Systems for Bridges, Structures, and Highways, Vol. 3325, SPIE, 1998, pp. 182–191, http://dx.doi.org/10.1117/12.310607.

[124] S. Kiggins, C.-M. Uang, Reducing residual drift of buckling-restrained braced frames as a dual system, Eng. Struct. 28 (11) (2006) 1525–1532, http://dx.doi.org/10.1016/j.engstruct.2005.10.023.

[125] R.I. Skinner, W.H. Robinson, G.H. McVerry, An Introduction to Seismic Isolation, Wiley, Hoboken, New Jersey, United States, 1993.

[126] D. Cardone, Re-centring capability of flag-shaped seismic isolation systems, Bull. Earthq. Eng. 10 (4) (2012) 1267–1284, http://dx.doi.org/10.1007/s10518-012-9343-1.

[127] R. Riddell, N.M. Newmark, Statistical analysis of the response of nonlinear systems subjected to earthquakes, Civ. Eng. Stud. Struct. Res. Ser. (University Illinois Urbana-Champaign) (1979).

[128] S.A. Mahin, V.V. Bertero, An evaluation of inelastic seismic design spectra, J. Struct. Div. 107 (9) (1981) 1777–1795, http://dx.doi.org/10.1061/JSDEAG.0005782.

[129] G. Rondelli, Corrosion resistance tests on NiTi shape memory alloy, Biomaterials 17 (20) (1996) 2003–2008, http://dx.doi.org/10.1016/0142-9612(95)00352-5.

[130] M. Es-Souni, M. Es-Souni, H. Fischer-Brandies, Assessing the biocompatibility of NiTi shape memory alloys used for medical applications, Anal. Bioanal. Chem. 381 (3) (2005) 557–567, http://dx.doi.org/10.1007/s00216-004-2888-3.

[131] A. Wadood, Brief overview on Nitinol as biomaterial, Adv. Mater. Sci. Eng. 2016 (2016) 1–9, http://dx.doi.org/10.1155/2016/4173138.

[132] C.D. Rovere, J. Alano, J. Otubo, S. Kuri, Corrosion behavior of shape memory stainless steel in acid media, J. Alloys Compd. 509 (17) (2011) 5376–5380, http://dx.doi.org/10.1016/j.jallcom.2011.02.051.

[133] C.D. Rovere, J. Alano, R. Silva, P. Nascente, J. Otubo, S. Kuri, Influence of alloying elements on the corrosion properties of shape memory stainless steels, Mater. Chem. Phys. 133 (2) (2012) 668–673, http://dx.doi.org/10.1016/j.matchemphys.2012.01.049.

[134] B. quan Hu, P. kang Bai, Z. zhong Dong, J. Chengd, Effect of Cu addition on corrosion resistance and shape memory effect of Fe-14Mn-5Si-9Cr-5Ni alloy, Trans. Nonferr. Met. Soc. China 19 (1) (2009) 149–153, http://dx.doi.org/10.1016/S1003-6326(08)60243-5.

[135] X. Huang, S. Chen, T.Y. Hsu, X. Zuyao, Corrosion behavior of Fe25Mn6Si5Cr shape memory alloys modified with rare earth in a NaCl solution, J. Mater. Sci. 39 (22) (2004) 6857–6859, http://dx.doi.org/10.1023/B:JMSC.0000045620.49206.6a.

[136] O. Söderberg, X. Liu, P. Yakovenko, K. Ullakko, V. Lindroos, Corrosion behaviour of Fe–Mn–Si based shape memory steels trained by cold rolling, Mater. Sci. Eng. A 273–275 (1999) 543–548, http://dx.doi.org/10.1016/S0921-5093(99)00396-2.

[137] H. Kuo, W. Wang, Y. Hsu, C. Huang, The corrosion behavior of Cu–Al and Cu–Al–be shape-memory alloys in 0.5M H2so4 solution, Corros. Sci. 48 (12) (2006) 4352–4364, http://dx.doi.org/10.1016/j.corsci.2006.04.006.

[138] E. Cesari, J. Pons, R. Santamarta, C. Segui, D. Stroz, H. Morawiec, Ageing effects in NiTi based shape memory alloys, Appl. Crystall. (2001) 171–185, http://dx.doi.org/10.1142/9789812811325_0024.

[139] V. Torra, A. Isalgue, F. Martorell, P. Terriault, F. Lovey, Built in dampers for family homes via SMA: An ANSYS computation scheme based on mesoscopic and microscopic experimental analyses, Eng. Struct. 29 (8) (2007) 1889–1902, http://dx.doi.org/10.1016/j.engstruct.2006.08.028.

[140] N. Suresh, U. Ramamurty, Aging response and its effect on the functional properties of Cu–Al–Ni shape memory alloys, J. Alloys Compd. 449 (1) (2008) 113–118, http://dx.doi.org/10.1016/j.jallcom.2006.02.094, The First International Symposium on Functional Materials (ISFM2005).

[141] L. Tseng, J. Ma, M. Vollmer, P. Krooß, T. Niendorf, I. Karaman, Effect of grain size on the superelastic response of a FeMnAlNi polycrystalline shape memory alloy, Scr. Mater. 125 (2016) 68–72, http://dx.doi.org/10.1016/j.scriptamat.2016.07.036.

[142] G. Wang, H. Peng, C. Zhang, S. Wang, Y. Wen, Relationship among grain size, annealing twins and shape memory effect in Fe–Mn–Si based shape memory alloys, Smart Mater. Struct. 25 (7) (2016) 075013, http://dx.doi.org/10.1088/0964-1726/25/7/075013.

[143] G.W. Housner, L.A. Bergman, T.K. Caughey, A.G. Chassiakos, R.O. Claus, S.F. Masri, R.E. Skelton, T.T. Soong, B.F. Spencer, J.T.P. Yao, Structural control: Past, present, and future, J. Eng. Mech. 123 (9) (1997) 897–971, http://dx.doi.org/10.1061/(ASCE)0733-9399(1997)123:9(897).

[144] K. Shiba, S. Mase, Y. Yabe, K. Tamura, Active/passive vibration control systems for tall buildings, Smart Mater. Struct. 7 (5) (1998) 588–598, http://dx.doi.org/10.1088/0964-1726/7/5/003.

[145] N. Makris, S.A. Burton, D. Hill, M. Jordan, Analysis and design of ER damper for seismic protection of structures, J. Eng. Mech. 122 (10) (1996) 1003–1011, http://dx.doi.org/10.1061/(ASCE)0733-9399(1996)122:10(1003).

[146] B.F. Spencer, S. Nagarajaiah, State of the art of structural control, J. Struct. Eng. 129 (7) (2003) 845–856, http://dx.doi.org/10.1061/(ASCE)0733-9445(2003)129:7(845).

[147] K. Wang, Y. Kim, D. Shea, Structural vibration control via electrorheological-fluid-based actuators with adaptive viscous and frictional damping, J. Sound Vib. 177 (2) (1994) 227–237, http://dx.doi.org/10.1006/jsvi.1994.1429.

[148] C. Liang, C.A. Rogers, One-dimensional thermomechanical constitutive relations for shape memory materials, J. Intell. Mater. Syst. Struct. 8 (4) (1997) 285–302, http://dx.doi.org/10.1177/1045389X9700800402.

[149] L. Brinson, One-dimensional constitutive behavior of shape memory alloys: Thermomechanical derivation with non-constant material functions and re-defined martensite internal variable, J. Intell. Mater. Syst. Struct. 4 (2) (1993) 229–242, http://dx.doi.org/10.1177/1045389X9300400213, URL http://journals.sagepub.com/doi/10.1177/1045389X9300400213.

[150] J. Boyd, D. Lagoudas, A thermodynamical constitutive model for shape memory materials. Part I. The monolithic shape memory alloy, Int. J. Plast. 12 (6) (1996) 805–842, http://dx.doi.org/10.1016/S0749-6419(96)00030-7.

[151] J.G. Boyd, D.C. Lagoudas, A thermodynamical constitutive model for shape memory materials. Part II. The SMA composite material, Int. J. Plast. 12 (7) (1996) 843–873, http://dx.doi.org/10.1016/S0749-6419(96)00031-9.

[152] H. Li, C.-X. Mao, J.-P. Ou, Strain self-sensing property and strain rate dependent constitutive model of austenitic shape memory alloy: Experiment and theory, J. Mater. Civ. Eng. 17 (6) (2005) 676–685, http://dx.doi.org/10.1061/(ASCE)0899-1561(2005)17:6(676).

[153] H. Tobushi, K. Takata, Y. Shimeno, W.K. Nowacki, S.P. Gadaj, Influence of strain rate on superelastic behaviour of TiNi shape memory alloy, Proc. Inst. Mech. Eng. Part L: J. Mater. Design Appl. 213 (2) (1999) 93–102, http://dx.doi.org/10.1177/146442079921300203.

[154] S. Sun, R. Rajapakse, Simulation of pseudoelastic behaviour of SMA under cyclic loading, Comput. Mater. Sci. 28 (3) (2003) 663–674, http://dx.doi.org/10.1016/j.commatsci.2003.08.022, Twelfth International Workshop on Computational Mechanics of Materials.

[155] F. Falk, Model free energy, mechanics, and thermodynamics of shape memory alloys, Acta Metall. 28 (12) (1980) 1773–1780, http://dx.doi.org/10.1016/0001-6160(80)90030-9.

[156] F. Falk, P. Konopka, Three-dimensional Landau theory describing the martensitic phase transformation of shape-memory alloys, J. Phys.: Condens. Matter 2 (1) (1990) 61–77, http://dx.doi.org/10.1088/0953-8984/2/1/005.

[157] E. Patoor, A. Eberhardt, M. Berveiller, Thermomechanical behavior of shape memory alloys, in: ESOMAT 1989 - Ist European Symposium on Martensitic Transformations in Science and Technology, EDP Sciences, Les Ulis, France, 1989, pp. 133–140, http://dx.doi.org/10.1051/esomat/198903002, URL http://www.esomat.org/10.1051/esomat/198903002.

[158] Q.P. Sun, K.C. Hwang, Micromechanics modelling for the constitutive behavior of polycrystalline shape memory alloys—I. Derivation of general relations, J. Mech. Phys. Solids 41 (1) (1993) 1–17, http://dx.doi.org/10.1016/0022-5096(93)90060-S.

[159] Q.P. Sun, K.C. Hwang, Micromechanics modelling for the constitutive behavior of polycrystalline shape memory alloys—II. Study of the individual phenomena, J. Mech. Phys. Solids 41 (1) (1993) 19–33, http://dx.doi.org/10.1016/0022-5096(93)90061-J.

[160] M. Huang, L. Brinson, A multivariant model for single crystal shape memory alloy behavior, J. Mech. Phys. Solids 46 (8) (1998) 1379–1409, http://dx.doi.org/10.1016/S0022-5096(97)00080-X.

[161] J.G. Boyd, D.C. Lagoudas, Thermodynamical constitutive model for the shape memory effect due to transformation and reorientation, in: V.K. Varadan (Ed.), Smart Structures and Materials 1994: Smart Materials, Vol. 2189, SPIE, International Society for Optics and Photonics, 1994, pp. 276–288, http://dx.doi.org/10.1117/12.174064.

[162] K. Wilde, P. Gardoni, Y. Fujino, Base isolation system with shape memory alloy device for elevated highway bridges, Eng. Struct. 22 (3) (2000) 222–229, http://dx.doi.org/10.1016/S0141-0296(98)00097-2.

[163] Y. Zhang, S. Zhu, A shape memory alloy-based reusable hysteretic damper for seismic hazard mitigation, Smart Mater. Struct. (2007) http://dx.doi.org/10.1088/0964-1726/16/5/014.
[164] W. Ren, H. Li, G. Song, A one-dimensional strain-rate-dependent constitutive model for superelastic shape memory alloys, Smart Mater. Struct. 16 (1) (2007) 191–197, http://dx.doi.org/10.1088/0964-1726/16/1/023.
[165] Y.-K. Wen, Method for random vibration of hysteretic systems, J. Eng. Mech. Div. 102 (2) (1976) 249–263, http://dx.doi.org/10.1061/JMCEA3.0002106.
[166] H. Ozdemir, Nonlinear Transient Dynamic Analysis of Yielding Structures, University of California, Berkeley, USA, 1976.
[167] A. Vitiello, G. Giorleo, R.E. Morace, Analysis of thermomechanical behaviour of Nitinol wires with high strain rates, Smart Mater. Struct. 14 (1) (2005) 215–221, http://dx.doi.org/10.1088/0964-1726/14/1/021.
[168] G. Song, N. Ma, H.-N. Li, Review of applications of shape memory alloys in civil structures, American Society of Civil Engineers, Reston, VA, 2004, pp. 559–566, http://dx.doi.org/10.1061/40722(153)78,
[169] M. Dolce, D. Cardone, R. Marnetto, Implementation and testing of passive control devices based on shape memory alloys, Earthq. Eng. Struct. Dyn. 29 (7) (2000) 945–968.
[170] Y. Liu, H. Wang, C. Qiu, X. Zhao, Seismic behavior of superelastic shape memory alloy spring in base isolation system of multi-story steel frame, Materials 12 (6) (2019) http://dx.doi.org/10.3390/ma12060997.
[171] B. Wang, S. Zhu, F. Casciati, Experimental study of novel self-centering seismic base isolators incorporating superelastic shape memory alloys, J. Struct. Eng. 146 (7) (2020) 04020129, http://dx.doi.org/10.1061/(ASCE)ST.1943-541X.0002679.
[172] F. Hedayati Dezfuli, M. Shahria Alam, Shape memory alloy wire-based smart natural rubber bearing, Smart Mater. Struct. 22 (4) (2013) 045013, http://dx.doi.org/10.1088/0964-1726/22/4/045013.
[173] F. Hedayati Dezfuli, M.S. Alam, Smart lead rubber bearings equipped with ferrous shape memory alloy wires for seismically isolating highway bridges, J. Earthq. Eng. 22 (6) (2018) 1042–1067, http://dx.doi.org/10.1080/13632469.2016.1269692.
[174] F. Hedayati Dezfuli, S. Li, M.S. Alam, J.-Q. Wang, Effect of constitutive models on the seismic response of an SMA-LRB isolated highway bridge, Eng. Struct. 148 (2017) 113–125, http://dx.doi.org/10.1016/j.engstruct.2017.06.036.
[175] F. Hedayati Dezfuli, M.S. Alam, Performance-based assessment and design of FRP-based high damping rubber bearing incorporated with shape memory alloy wires, Eng. Struct. 61 (2014) 166–183, http://dx.doi.org/10.1016/j.engstruct.2014.01.008.
[176] A.B. Habieb, M. Valente, G. Milani, Hybrid seismic base isolation of a historical masonry church using unbonded fiber reinforced elastomeric isolators and shape memory alloy wires, Eng. Struct. 196 (2019) 109281, http://dx.doi.org/10.1016/j.engstruct.2019.109281.
[177] K. Varughese, R. El-Hacha, Experimental free vibrations test of steel braced frames reinforced with NiTi shape memory alloy wires, Structures (2021) http://dx.doi.org/10.1016/j.istruc.2020.11.022.
[178] R. Kamgar, H. Heidarzadeh, M.R. Babadaei Samani, Evaluation of buckling load and dynamic performance of steel shear wall retrofitted with strips made of shape memory alloy, Sci. Iran. 28 (3) (2021) 1096–1108, http://dx.doi.org/10.24200/sci.2020.52994.2991.
[179] B. Wang, S. Zhu, C.X. Qiu, H. Jin, High-performance self-centering steel columns with shape memory alloy bolts: Design procedure and experimental evaluation, Eng. Struct. (2019) http://dx.doi.org/10.1016/j.engstruct.2018.12.077.
[180] D. Cardone, R. Angiuli, G. Gesualdi, Application of shape memory alloys in historical constructions, Int. J. Archit. Heritage 13 (3) (2019) 390–401, http://dx.doi.org/10.1080/15583058.2018.1563225.
[181] H. Dong, X. Du, Q. Han, Seismic responses of steel frame structures with self-centering energy dissipation braced on shape memory alloy cables, Adv. Struct. Eng. 22 (9) (2019) 2136–2148, http://dx.doi.org/10.1177/1369433219834752.
[182] B. Wang, S. Zhu, Seismic behavior of self-centering reinforced concrete wall enabled by superelastic shape memory alloy bars, Bull. Earthq. Eng. 16 (1) (2018) 479–502, http://dx.doi.org/10.1007/s10518-017-0213-8.
[183] N. Mirzai, R. Attarnejad, Seismic performance of EBFs equipped with an innovative shape memory alloy damper, Sci. Iran. 27 (5) (2020) 2316–2325, http://dx.doi.org/10.24200/sci.2018.50990.1955.
[184] M. Mahmoudi, S. Montazeri, M.J. Sadr Abad, Seismic performance of steel X-knee-braced frames equipped with shape memory alloy bars, J. Construct. Steel Res. 147 (2018) 171–186, http://dx.doi.org/10.1016/j.jcsr.2018.03.019.
[185] K. Hong, S. Lee, Y. Yeon, K. Jung, Flexural response of reinforced concrete beams strengthened with near-surface-mounted Fe-based shape-memory alloy strips, Int. J. Concrete Struct. Mater. 12 (1) (2018) 45, http://dx.doi.org/10.1186/s40069-018-0279-y.
[186] A. Abbass, R. Attarnejad, M. Ghassemieh, Seismic assessment of RC bridge columns retrofitted with near-surface mounted shape memory alloy technique, Materials 13 (7) (2020) http://dx.doi.org/10.3390/ma13071701.
[187] K. Ke, X. Zhou, M. Zhu, M.C. Yam, Y. Wang, H. Zhang, Seismic evaluation of industrial steel moment resisting frames with shape memory alloys using performance-spectra-based method, J. Build. Eng. 48 (2022) 103950, http://dx.doi.org/10.1016/j.jobe.2021.103950.
[188] B. Chen, X. Song, W. Li, J. Wu, Vibration control of a wind-excited transmission tower-line system by shape memory alloy dampers, Materials 15 (5) (2022) http://dx.doi.org/10.3390/ma15051790.
[189] F.A. Nae, T. Ikeda, Y. Matsuzaki, The active tuning of a shape memory alloy pseudoelastic property, Smart Mater. Struct. 13 (3) (2004) 503–511, http://dx.doi.org/10.1088/0964-1726/13/3/008.
[190] C.A. Rogers, Active vibration and structural acoustic control of shape memory alloy hybrid composites: Experimental results, J. Acoust. Soc. Am. 88 (6) (1990) 2803–2811, http://dx.doi.org/10.1121/1.399683.
[191] Q. Chen, C. Levy, Active vibration control of elastic beam by means of shape memory alloy layers, Smart Mater. Struct. 5 (4) (1996) 400–406, http://dx.doi.org/10.1088/0964-1726/5/4/003.
[192] A.R. Shahin, P.H. Meckl, J.D. Jones, Modeling of SMA tendons for active control of structures, J. Intell. Mater. Syst. Struct. 8 (1) (1997) 51–70, http://dx.doi.org/10.1177/1045389X9700800106.
[193] K. Williams, G. Chiu, R. Bernhard, Adaptive-passive absorbers using shape-memory alloys, J. Sound Vib. 249 (5) (2002) 835–848, http://dx.doi.org/10.1006/jsvi.2000.3496.
[194] A. Baz, K. Imam, J. McCoy, Active vibration control of flexible beams using shape memory actuators, J. Sound Vib. 140 (3) (1990) 437–456, http://dx.doi.org/10.1016/0022-460X(90)90760-W.
[195] P. Vishal, D. Kaliperumal, R. Padhi, Active vibration suppression of nonlinear cantilever beam using shape memory alloy actuators, IFAC-PapersOnLine 51 (1) (2018) 130–135, http://dx.doi.org/10.1016/j.ifacol.2018.05.022, 5th IFAC Conference on Advances in Control and Optimization of Dynamical Systems ACODS 2018.
[196] Y. Suzuki, Y. Kagawa, Active vibration control of a flexible cantilever beam using shape memory alloy actuators, Smart Mater. Struct. 19 (8) (2010) 085014, http://dx.doi.org/10.1088/0964-1726/19/8/085014.
[197] S.S. Nakshatharan, D.J.S. Ruth, K. Dhanalakshmi, Design based active vibration control of a flexible structure using shape memory alloy wire actuators, in: 2012 Sixth International Conference on Sensing Technology, ICST, 2012, pp. 476–480, http://dx.doi.org/10.1109/ICSensT.2012.6461725.
[198] K. Alambeigi, M. Mohammadimehr, M. Bamdad, T. Rabczuk, Free and forced vibration analysis of a sandwich beam considering porous core and SMA hybrid composite face layers on Vlasov's foundation, Acta Mech. 231 (8) (2020) 3199–3218, http://dx.doi.org/10.1007/s00707-020-02697-5.
[199] J. Heinonen, I. Vessonen, P. Klinge, E. Järvinen, Controlling stiffness of a frame spring by changing the boundary condition with an SMA actuator, Comput. Struct. 86 (3) (2008) 398–406, http://dx.doi.org/10.1016/j.compstruc.2007.02.008, Smart Structures.
[200] C. Cismasiu, F.P.A. Dos Santos, Numerical simulation of a semi-active vibration control device based on superelastic shape memory alloy wires, in: Shape Mem. Alloy., 2010, http://dx.doi.org/10.5772/9963.
[201] S.K. Mishra, S. Gur, S. Chakraborty, An improved tuned mass damper (SMA-tmd) assisted by a shape memory alloy spring, Smart Mater. Struct. 22 (9) (2013) 095016, http://dx.doi.org/10.1088/0964-1726/22/9/095016.
[202] S. Zareie, A. Zabihollah, A semi-active SMA-MRF structural stability element for seismic control in marine structures, Appl. Ocean Res. 100 (2020) 102161, http://dx.doi.org/10.1016/j.apor.2020.102161.
[203] S. Zareie, M. Hamidia, A. Zabihollah, R. Ahmad, K.M. Dolatshahi, Design, validation, and application of a hybrid shape memory alloy-magnetorheological fluid-based core bracing system under tension and compression, Structures 35 (2022) 1151–1161, http://dx.doi.org/10.1016/j.istruc.2021.08.094.
[204] K. Kecik, Numerical study of a pendulum absorber/harvester system with a semi-active suspension, ZAMM - J. Appl. Math. Mech. / Zeitschrift Für Angew. Math. Und Mech. 101 (1) (2021) http://dx.doi.org/10.1002/zamm.202000045.
[205] H. Huang, W.-S. Chang, Application of pre-stressed SMA-based tuned mass damper to a timber floor system, Eng. Struct. 167 (2018) 143–150, http://dx.doi.org/10.1016/j.engstruct.2018.04.011.
[206] H. Zuo, K. Bi, H. Hao, C. Li, Numerical study of using shape memory alloy-based tuned mass dampers to control seismic responses of wind turbine tower, Eng. Struct. 250 (2022) 113452, http://dx.doi.org/10.1016/j.engstruct.2021.113452.
[207] Z.-X. Zhang, Y. Ping, X. He, Self-centering shape memory alloy-viscoelastic hybrid braces for seismic resilience, Materials 15 (2022) http://dx.doi.org/10.3390/ma15072349.
[208] F.H. Dezfuli, M.S. Alam, Smart lead rubber bearings equipped with ferrous shape memory alloy wires for seismically isolating highway bridges, J. Earthq. Eng. 22 (6) (2018) 1042–1067, http://dx.doi.org/10.1080/13632469.2016.1269692.
[209] F. Shi, Y. Zhou, O.E. Ozbulut, S. Cao, Development and experimental validation of anchorage systems for shape memory alloy cables, Eng. Struct. (2021) http://dx.doi.org/10.1016/j.engstruct.2020.111611.
[210] R. Suhail, G. Amato, D. McCrum, Active and passive confinement of shape modified low strength concrete columns using SMA and FRP systems, Compos. Struct. 251 (2020) 112649, http://dx.doi.org/10.1016/j.compstruct.2020.112649.
[211] S. Zareie, A.S. Issa, R. Seethaler, A. Zabihollah, R. Ahmad, A novel SMA-magnetorheological hybrid bracing system for seismic control, Eng. Struct. 244 (2021) 112709, http://dx.doi.org/10.1016/j.engstruct.2021.112709.

[212] G. Song, B. Kelly, B.N. Agrawal, Active position control of a shape memory alloy wire actuated composite beam, Smart Mater. Struct. 9 (5) (2000) 711–716, http://dx.doi.org/10.1088/0964-1726/9/5/316.

[213] M. Sreekumar, M. Singaperumal, T. Nagarajan, M. Zoppi, R. Molfino, Recent advances in nonlinear control technologies for shape memory alloy actuators, J. Zhejiang Univ.-Sci. A 8 (5) (2007) 818–829, http://dx.doi.org/10.1631/jzus.2007.A0818.

[214] J. McCormick, R. DesRoches, D. Fugazza, F. Auricchio, Seismic assessment of concentrically braced steel frames with shape memory alloy braces, J. Struct. Eng. 133 (6) (2007) 862–870, http://dx.doi.org/10.1061/(ASCE)0733-9445(2007)133:6(862).

[215] G.L. McGavin, G. Guerin, Real-time seismic damping and frequency control of steel structures using nitinol wire, in: S.-C. Liu, D.J. Pines (Eds.), Smart Structures and Materials 2002: Smart Systems for Bridges, Structures, and Highways, Vol. 4696, SPIE, International Society for Optics and Photonics, 2002, pp. 176–185, http://dx.doi.org/10.1117/12.472553.

[216] J.P. Amezquita-Sanchez, A. Dominguez-Gonzalez, R. Sedaghati, R. de Jesus Romero-Troncoso, R.A. Osornio-Rios, Vibration control on smart civil structures: A review, Mech. Adv. Mater. Struct. 21 (1) (2014) 23–38, http://dx.doi.org/10.1080/15376494.2012.677103.